Global Analysis, Interpretation and Modelling
An Earth Systems Modelling Program

FINAL REPORT
NASA GRANT # NAGW 4706

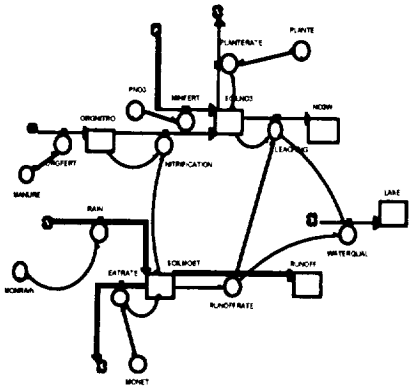

African-GAIM Modelling Workshop

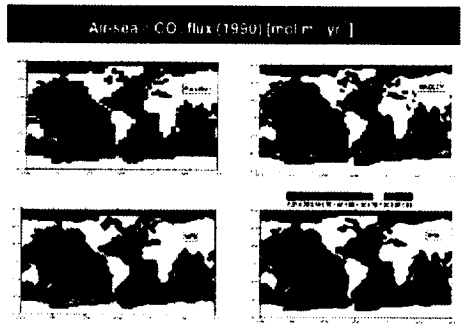

Comparison of 4 OCMIP model simulations of STELLA model air-sea CO_2 flux.

Submitted by:
Berrien Moore III
Director
Institute for the Study of Earth, Oceans, and Space

Dork Sahagian
Executive Director
Global Analysis, Interpretation, and Modelling Task Force
International Geosphere Biosphere Program

December 1997

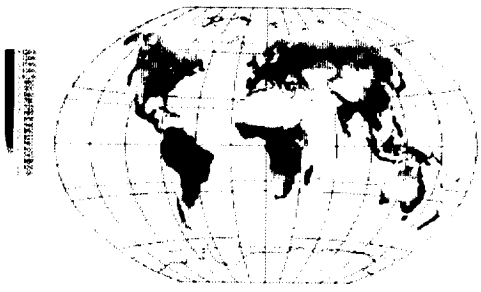

Global mean Net Primary Productivity, showing averaged results of 17 models compared at the 1995 NPP workshop in Potsdam, Germany.

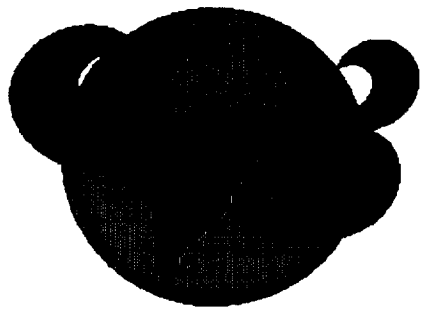

Atmospheric Tracer Transport

Final Report on GAIM activities

The role of the IGBP Task Force on Global Analysis, Interpretation, and Modelling (GAIM) is multi-fold. The Task Force must analyze current models and data, interpret the capability of current models and experimental programs against the demands for knowledge, and advance and synthesize our understanding of the global biogeochemical cycles and their links to the hydrological cycle and more generally to the physical-climate system as a whole.

Modelling is fundamental to the IGBP effort because the ability to model some aspect of the Earth system correctly and repeatedly on the basis of component processes is a litmus test of whether or not predictive understanding of that component has been achieved. Models also provide an indispensable way of organizing current knowledge and pinpointing critical gaps. The aim is not simply to produce ever larger and more complex models of the Earth, but rather to produce a family of models of varying complexity and realism to attack specific questions. The models and model experiments have to be designed in such a way that their predictive characteristics can be tested with existing or planned (generally historical) data sets.

General Circulation Models exist at a variety of institutions around the world; prognostic Global Biogeochemical Models are at a relatively primitive stage. The challenge to GAIM is to initiate activities that will lead to the rapid development and application of a suite of Global Biogeochemical Models. These Global Biogeochemical Models would, in time, be linked, partly through the hydrological coupling, to General Circulation Models, thereby, providing models of the Earth system.

The Goal of the GAIM is:

> ***•To advance the study of the coupled dynamics of the Earth system using as tools both data and models.***

GAIM emphasizes activities designed to expand upon the development, testing, and analyses of integrative data sets and models of those aspects of the Earth system where the IGBP program has the scientific lead, and works in collaboration on aspects of the Earth system where WCRP programs have the lead. GAIM is working with IGBP Core Projects to identify appropriate component models, to assist in integrating these into coupled models, and to test and apply these coupled models. The integration, testing, and analysis of coupled models will generate specific requirements for data: for initialization, forcing, and validation. Development of these data sets is being coordinated through IGBP-DIS.

In order to make progress toward this goal, the IGBP Task Force for Global Analysis, Interpretation, and Modelling has established the following specific objectives:

> ***•To develop a strategy for the rapid development, evaluation, and application of comprehensive prognostic models of the Global Biogeochemical Subsystem which could eventually be linked with models of the Physical-Climate Subsystem.***
>
> ***•To propose, promote, and facilitate experiments with existing models or by linking subcomponent models, especially those associated with IGBP Core Projects and with WCRP efforts. Such experiments would be focused upon resolving interface issues and questions associated with developing an understanding of the prognostic behavior of key processes.***
>
> ***•To clarify key scientific issues facing the development of Global Biogeochemical Models and the coupling of these models to General Circulation Models.***
>
> ***•To assist the Intergovernmental Panel on Climate Change (IPCC) process by conducting timely studies that focus upon elucidating important unresolved scientific issues associated***

with the changing biogeochemical cycles of the planet and upon the role of the biosphere in the physical-climate subsystem, particularly its role in the global hydrological cycle.

•To advise the SC-IGBP on progress in developing comprehensive Global Biogeochemical Models and to maintain scientific liaison with the WCRP Steering Group on Global Climate Modelling.

During the first phase, the focal biogeochemical cycle for GAIM has been the carbon cycle, including its interaction with aspects of the nitrogen cycle. Coupled analyses of feedbacks between dynamic biogeochemistry and climate, mediated by greenhouse gas concentrations, and of climate-ecosystem interactions mediated by the hydrological cycle are being initiated by GAIM and, where appropriate, conducted in collaboration with WCRP programs.

AFRICAN-GAIM MODELLING WORKSHOP

March 3-12, 1997, Mombasa, Kenya

OVERVIEW

GAIM emphasizes activities designed to expand upon the development, testing, and analyses of integrative data sets and models of those aspects of the Earth system where the IGBP program has the scientific lead, and works in collaboration on aspects of the Earth system where World Climate Research Program (WCRP) has the lead. GAIM collaborates with IGBP Core Projects in identifying appropriate component models, in assisting in the integration of these into coupled models, and in testing and applying these coupled models. The integration, testing, and analysis of coupled models generates specific requirements for data: for initialization, forcing, and validation. Development of these data sets is coordinated through IGBP Data and Information Systems (DIS).

The global environmental issues that the IGBP is seeking to understand confront all regions: they hold a particular challenge for developing regions where growing populations may intersect increasing rates of environmental change. Many tropical regions display both the causes of global change (e.g. biomass burning) and their effects (e.g. variations in precipitation patterns). These cause-effect systems offer not only an environmental challenge but also a scientific opportunity to understand better the relationship between human society and the biosphere. In addition, these regions hold important records of past environmental change that are important if we are to test models and ideas about future environmental change. Finally, in many developing regions there is not yet an adequate scientific or policy community to participate fully in the global environment policy process (e.g. the Intergovernmental Panel on Climate Change (IPCC)). These considerations offer a challenge to IGBP, to the IGBP Core Projects, to the IGBP GAIM Task Force, and to the IGBP-DIS effort. In part, Global Change System for Analysis, Research, and Training (START) and the European Network for Research In Global Change (ENRICH) were created to facilitate the IGBP and its sister Programs, the World Climate Research Programme (WCRP) and the International Human Dimensions Programme (IHDP), in meeting this challenge.

The African-GAIM Modelling Workshop was directed toward:

- Analyzing key models and data with particular relevance to Africa,
- Interpreting the capability of these models to describe system processes within the region, and validation with field data,
- Building the international modelling and data infrastructures needed to support fully the IPCC process,
- Expanding the capability within Africa to use models focused upon key topics within the overall theme of global change, including
  - -the effect of land use change on carbon and nutrient cycling in terrestrial ecosystems, and
  - -water cycling and water management.
- Developing model applications to problems associated with land use changes and sustainability of African agricultural and other land use.

The Workshop focused on models applicable to Africa in the global context, including terrestrial ecosystem and hydrologic models. Hydrological and ecological models were presented, run by participants in hands-on "laboratory" sessions, and interpreted in terms of African and global applications. Participants developed their own modelling projects during the workshop, to be subsequently expanded at their home institutions as part of broader African global change modelling community. The intent was to include as many younger scientists as possible.

Participants divided into two parallel sessions with one focusing on hydrologic models while and the other on ecological models. These models were presented by their developers, and workshop participants were given hands-on experience in running and manipulating the models and their results. Subsequently, a simple box-modelling program was introduced to give the participants the opportunity to recreate certain aspects of the hydro- and eco- models as well as to create their own models in real time at the workshop. The final phase of the workshop was a team effort by participant groups to

develop a project or pose a tractable problem for collaborative research in the months following the workshop. These included some which represented extension of existing African IGBP programs as well as new projects which were formulated at the workshop. The participant presentations highlighted the fact that there is a great deal of research expertise throughout Africa. There are also numerous international research programs being conducted throughout Africa, some within the auspices of IGBP.

A special session was held for discussion of issues impacting the African global change research community. Of these, two issues emerged as primary- resources, and human impacts. It was clear from the start of the workshop that in many institutions throughout Africa, there are insufficient resources to conduct the research needed to support an African modelling community. In particular, even the most basic computing facilities are often lacking. It was determined that this problem could best be solved in the context of active research projects. In the course of collaborative funded research, the necessary resources for modelling projects would become available. The workshop participants are formulating research projects in the months following the workshop. The second issue was the importance of human impacts of global change to the African research community. In most regions in Africa, there is considerable concern regarding the ability of current and projected food production systems to provide sufficiently for the growing population in the face of changing and variable climate conditions. A significant aspect of the workshop was to prepare the participants to return to their home institutions with the modelling exposure that will enable them to help build a stronger, more integrated African modelling community. In addition, the participants will act as a knowledge base for further education and capacity building within the African universities and research community in the coming years.

The African-GAIM Modelling Workshop was a first step in augmenting the African global change modelling community. In considering future workshops, it was agreed by the participants that while the format for this first activity was an appropriate beginning, the next gathering should be based on the presentation of concrete results from modelling projects which emerged from the workshop. The participants will keep in contact with each other and with GAIM in the meantime throughout the development, funding and implementation of their projects. A major set of presentations is planned for the SAC-V meeting in Nairobi in September, 1998.

PARTICIPANT PRESENTATIONS

Each of the participants in the African-GAIM Modelling Workshop brought to the meeting a large body of knowledge and research results. In order to best integrate the ongoing research throughout Africa with the modelling exercises at the workshop, each participant made a 10-minute presentation of his/her own recent research results. The breadth of topics covered highlighted the fact that there is a wealth of research expertise throughout Africa, and that GAIM and IGBP can benefit greatly from enhanced interaction and international collaboration (See Appendix 1).

WORKSHOP PARTICIPANT MODELLING PROJECT SUMMARIES AND STELLA MODELS

An introduction was presented by Dork Sahagian on the STELLA modelling package, a convenient graphical box model developer. Using STELLA, it is possible to conceptually construct a simple system model with the relevant stocks (reservoirs) and fluxes (exchanges between reservoirs) of various entities such as carbon, trees, elephants, people, money, etc. The fluxes are specified by equations relating the various stocks, constants, and various functions determined by the models which then graphically display the changes in the stocks and values of fluxes as a function of time during a model run. While it is exceedingly simple to construct a model in this way, a stumbling block that appeared throughout the workshop was that the participants did not know the appropriate constants and functions to specify in formulating the equations for the fluxes. This directly highlighted the gaps in scientific understanding of the systems they were modelling. While STELLA and other models can

describe a system conceptually, in order to accurately apply the model, it is necessary to quantify the relationships between system parameters. This caused workshop participants to think back to their systems and consider the types of field campaigns and other research that would be necessary to quantify these relationships. This was probably the most important result of the workshop because it clearly demonstrated the utility and limitations of modelling techniques, as demonstrated with models developed by the participants (See Appendix 2).

The workshop participants formed groups of three to four to construct models using the STELLA modelling package. In forming groups, the rule was to include at least one participant who specialized in hydrologic problems and one who specialized in ecological problems. The groups were multinational and multidisciplinary and resulted in the simple models (examples shown in Appendix 3).

OCEAN CARBON-CYCLE MODEL INTERCOMPARISON PROJECT (OCMIP)

PHASE I: INITIAL RESULTS

INTRODUCTION

The addition of carbon dioxide to the atmosphere through fossil fuel burning and deforestation is an inadvertent global experiment, the outcome of which has profound implications for the future of the earth's climate and hence for humankind itself. Society is looking toward the community of Global Change researchers to predict the outcome of this experiment so that sound input can be provided to economists, environmental engineers, and, ultimately, policy makers. One millennium from now, long after all fossil fuel supplies will have been exhausted, the ocean will have absorbed and retained about 7 out of every 8 molecules of anthropogenic CO_2 ever emitted to the atmosphere. Confidence in this prediction comes from the agreement between related simulations in global ocean, carbon-cycle models, from the simplest (which divides the ocean into a few boxes) to the most complex (which contains many thousands of grid cells). Less confidence can be given to any one model's prediction about more immediate changes, e.g., over the next couple of centuries. Also less agreement exists concerning today's regional uptake patterns, as well as those during other times. Models differ substantially even without consideration of potential changes in ocean circulation and possible shifts in the composition of oceanic plankton, much less the large uncertainty in future emissions of anthropogenic CO_2. Marine carbon cycle models have provided important constraints on the large-scale patterns of the marine uptake of anthropogenic CO_2 [*Maier-Reimer et al.*, 1996; *Sarmiento et al.*, 1992; *Siegenthaler and Sarmiento*, 1993], new production [*Bacastow and Stegen*, 1991; *Najjar et al.*, 1992], and remineralization, three important fluxes that have largely been elusive to direct observation over large spatial scales.

Consequently, the challenge to oceanographers is to synthesize the available data sets and incorporate into models that can be used for simulation of the partitioning of CO_2 between the atmosphere and the ocean. GAIM is responding to that challenge in the Ocean Carbon-Cycle Model Intercomparison Project (OCMIP), a coordinated effort of *evaluation* and *intercomparison* of 3-D global marine carbon cycle models.

Evaluation of marine carbon cycle models using observations of carbon-system and related parameters is necessary in order to establish the reliability of using such models for future prediction. A highly simplified "perturbation" approach, in which the natural carbon cycle and its attendant biological complexity are ignored, is feasible if ocean circulation and biogeochemistry can be assumed as invariant. [*Siegenthaler and Sarmiento*, 1993]. However, there are many indications that the earth's climate and ocean circulation are indeed changing and may change dramatically in the future [*Manabe and Stouffer*, 1994]. In that case, the potential for complex marine biogeochemical feedbacks is large [*Sarmiento and LeQuere*, 1996], and we are therefore behooved to develop the capability to model those aspects of the natural marine carbon cycle that are relevant to the air-sea partitioning of carbon dioxide. There are important data sets being compiled such as those by the Joint Global Ocean Flux Study (JGOFS), the next generation of satellite ocean color products, and a number of existing seasonal, global scale syntheses of nutrients [*Conkright and Asem*, 1995], dissolved oxygen [*Levitus and Boyer*, 1994; *Najjar and Keeling*, 1997], surface carbon dioxide [*Takahashi et al.*, 1997] and chlorophyll [*Banse and English*, 1994; *Yoder et al.*, 1993]. These data present an unprecedented opportunity for the evaluation of models of the natural marine carbon cycle.

During the first phase of intercomparison, OCMIP's focus was to identify differences between simulations of both natural and anthropogenic CO_2 in four 3-D models: from Max Planck Institut fur Meteorologie (MPIM, Germany), Princeton University/GFDL (USA), Hadley Centre (U.K. Met. Office), and IPSL/CFR-LMCE-LODyC (France). Sice that time, several additional models have been

added (Appendix). Additionally, OCMIP compares measured vs. simulated C-14 (for both natural and bomb components, separately) as a means to validate the model circulation fields which drive each of the four carbon-cycle models.

Results show that although the models all have the same overall pattern of enhanced uptake in upwelling and convective regions and weak uptake in downwelling regions, there are dramatic regional differences among the models, particularly in the Southern Ocean. Dramatic differences between model and observations are seen in the Southern Ocean, with the model overestimating the uptake of anthropogenic CO_2. Because this region of the ocean plays a critical role in determining atmospheric CO_2, these results are now provoking the careful evaluation of the models with relevant observations and the identification of the processes that cause such differences among the models.

OBJECTIVES

The long-term objectives of OCMIP are:

(1) To improve 3-D marine carbon cycle models for their use in predicting the future partitioning of carbon dioxide between the atmosphere and the ocean

(2) To make estimates of important but poorly-known quantities that are relevant to the marine carbon cycle: new production, aphotic zone remineralization and anthropogenic CO_2 fluxes and inventories

Since the above objectives require an understanding of the natural marine carbon cycle and its anthropogenic perturbation, both of which are profoundly influenced by ocean circulation, OCMIP defined the following shorter-term objectives:

(1) To evaluate and intercompare the ability of 3-D global models to simulate the natural marine carbon cycle

(2) To evaluate and intercompare the ability of 3-D global models to simulate the marine uptake of anthropogenic CO_2

(3) To evaluate and intercompare those aspects of the ocean circulation that are relevant to the natural marine carbon cycle and its anthropogenic perturbation

To achieve these objectives OCMIP has been running a series of simulations (Table 1), most of which are designed so that they may be readily evaluated with existing data sets.

Table 1: OCMIP simulations.

1. Natural marine carbon cycle
Biological plus solubility pump (PO_4, O_2 and DIC)
Nutrient-restoring model
Individual investigator model
Solubility pump only (DIC only)
2. Anthropogenic marine carbon cycle
1750-present
IPCC scenario S450
IPCC scenario S650
Pulse input

3. Tracers of ocean circulation
CFC-11
CFC-12
Natural radiocarbon
Bomb radiocarbon

Oceanic Uptake and Storage of CO_2

The ocean is by far the largest active reservoir of carbon on earth. Most anthropogenic CO_2 will one day be stored there, despite relatively slow oceanic uptake which cannot keep pace with excess CO_2 emissions to the atmosphere. Ocean models offer the most appropriate means to estimate past and present oceanic uptake of anthropogenic CO_2, and they provide the only option to predict future changes. Simplistic calculations have shown that about 7 out of every 8 molecules of anthropogenic CO_2 emitted to the atmosphere will eventually reside in the ocean; and the same result is found by making idealized simulations in 3-D models. But, however, these simulations do not consider additional uncertainties due to changes in ocean circulation, chemistry, and biology [*Maier-Reimer et al.*, 1996; *Sarmiento and LeQuere*, 1996]. Even without these complications transient uptake by the ocean is poorly constrained, particularly at the regional level. Previous results have demonstrated that model predictions of today's air-sea flux of anthropogenic CO_2 differ by 20% globally, but they differ by nearly a factor of two in the Southern Ocean, the largest sink. With time, as the Southern Ocean sink absorbs proportionally even more (relative to other regions), global differences between models will grow. OCMIP aims to better constrain our understanding of CO_2 uptake by the ocean, the major long-term sink, through standardized validation and comparison of independently developed ocean models.

Tracer Validation of Ocean Model Used to Estimate Ocean Storage of Anthropogenic CO_2

Model evaluation (often referred to as validation) is critical to any exercise where model predictions are to be taken seriously. OCMIP evaluates the behavior of ocean models by comparing their simulated distributions of appropriate tracers to measurements taken in the real ocean. The tracers of the greatest interest to our first objective (storage of anthropogenic CO_2) are bomb ^{14}C and CFC's, which like anthropogenic CO_2 are of a transient nature and have invaded only near-surface waters. One benefit to using both these tracers is that their surface-ocean/atmosphere equilibration times bracket that for anthropogenic CO_2. Participating models by using two very different tracers of deep-ocean circulation: natural ^{14}C and ^{3}He. Natural ^{14}C is produced cosmogenically in the upper atmosphere, is rapidly attached to molecules of CO_2, and is transferred to the ocean through gas exchange at air-sea interface; ^{3}He is unique in that its only supply is from the ocean floor along mid-ocean ridges.

When a model fails validation, it should ideally be adjusted then revalidated (Fig. 1 and Fig. 2). This calibration loop should be repeated as necessary, usually many times to make the model as realistic as possible. For 3-D ocean models, however, such an undertaking is difficult, long, and costly. By standardizing protocols and analysis, and by developing an integrated analysis package, which is freely distributable, OCMIP has automated the task of calibrating 3-D ocean models.

RESULTS OF MODEL INTERCOMPARISONS

Natural CO_2

Since preindustrial times, the rise in atmospheric CO_2 has caused the change in the air-to-sea CO_2 flux to be positive everywhere. This perturbation to the natural system, termed anthropogenic CO_2, is difficult to measure in the ocean. Four OCMIP models have been used to estimate oceanic uptake of anthropogenic CO_2 (Fig. 1). Although models agree to within 20% for global uptake of anthropogenic CO_2 during the 1980's (Table 2), regional uptake can differ by much more.

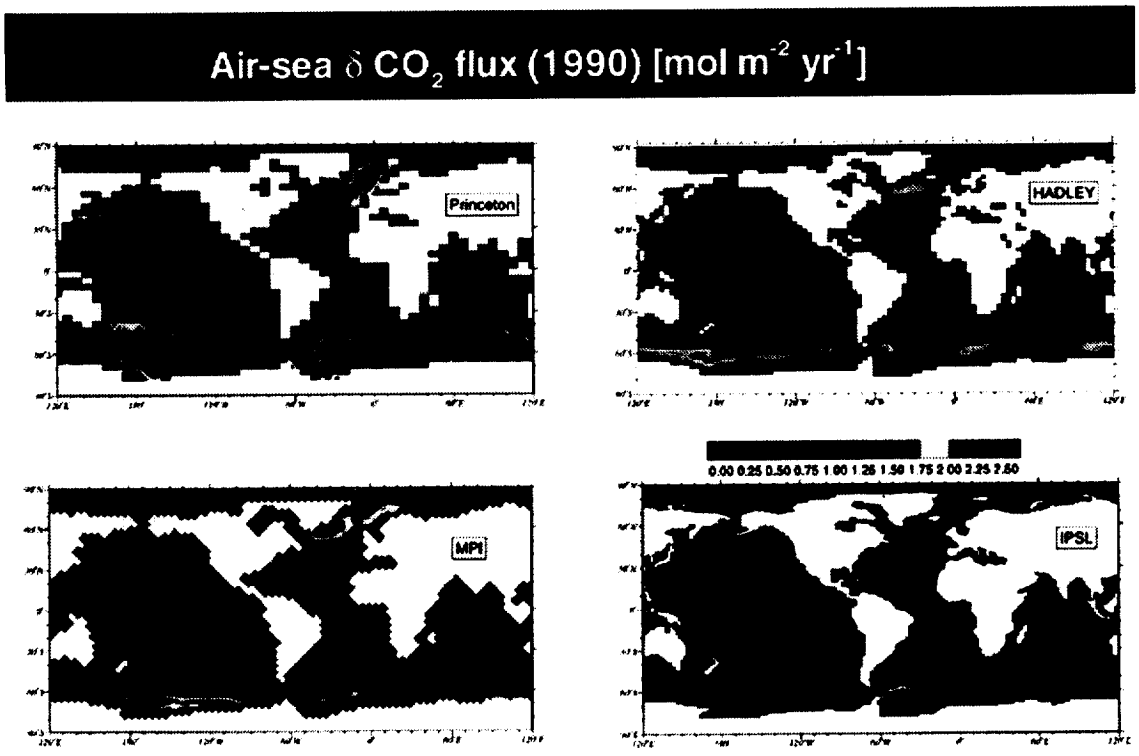

Figure 1
Comparison of 4 OCMIP model simulations of air-sea CO_2 flux.

Table 2: Anthropogenic CO_2 Uptake (1980--1989)

Model	Uptake [Pg C yr^{-1}]
GFDL/Princeton	2.2
HADLEY	2.1
IPSL	1.5
MPIM	1.6

Ocean uptake is highest in the high latitudes and at the equator (Fig. 2), i.e., in zones where deep waters uncontaminated with anthropogenic CO_2 communicate readily with the surface (via upwelling and convection). The Southern Ocean dominates as the major sink also because of its large surface area. Models differ by more than 100% in their predictions of how much anthropogenic CO_2 is absorbed in the Southern Ocean. Additionally, the predicted position of maximum uptake in the same region differs between models by nearly 20%.

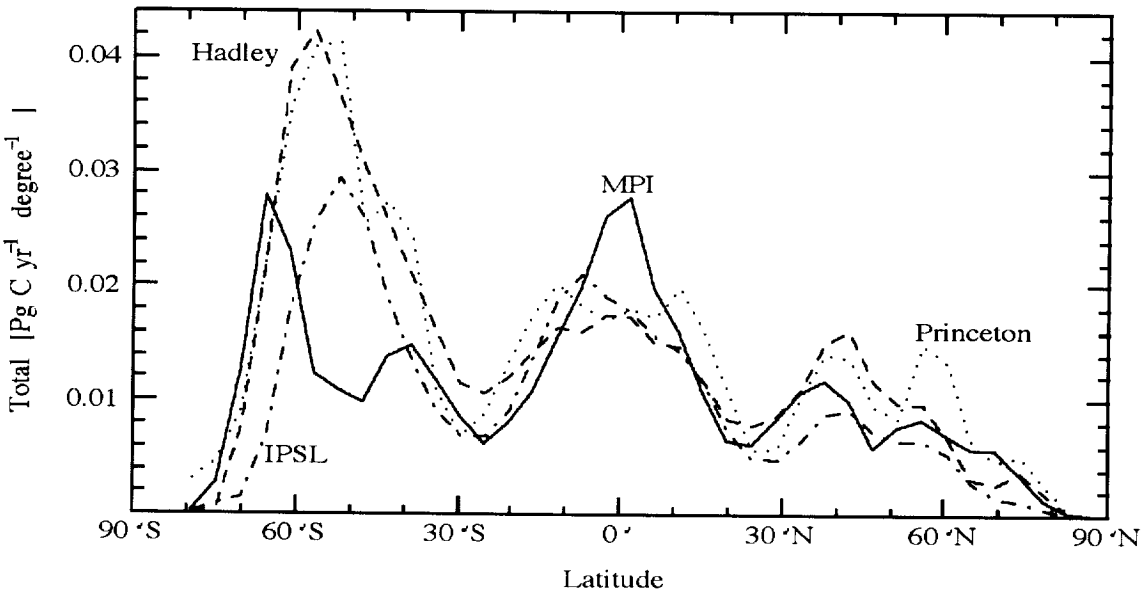

Figure 2
Global ocean, zonal mean air-to-sea flux of anthropogenic CO_2 given in Pg C yr-1 degree-1 as calculated by four OCMIP models for 1990. The oceanic uptake per band of latitude is most important in the Southern Ocean, but even there predictions vary considerably between models, both in the total absorbed and in the position of maximum absorption.

Simulations differ most in the Southern Ocean for natural CO_2, as well. OCMIP simulates the natural carbon cycle in order to properly validate ocean carbon-cycle models with ocean CO_2 measurements as well as to better constrain our understanding of the partitioning of CO_2 between the terrestrial biosphere and the ocean. Uncertainties in the latter are perhaps best exemplified by discrepancies between predictions from ocean models vs. those from atmospheric models which use observed distributions of CO_2 and C-13 in the atmosphere to back out present-day carbon fluxes to and from the atmosphere [*Ciais et al.*, 1995; *Tans et al.*, 1990].

For the natural carbon cycle, OCMIP separately runs simulations to distinguish effects due to the two major processes, which along with ocean circulation control the distribution of natural CO_2. The first relates to the temperature-dependent solubility of CO_2. The cold waters which fill the deep ocean from the high latitudes are rich in CO_2. Secondly, ocean biota act to reduce surface ocean CO_2 through the combined action of planktonic uptake, rapid transport to depth of resulting particulate organic carbon, and subsequent bacterial degradation. We denote these two processes as the solubility and biological pumps, respectively [*Volk*, 1988].

Although temperature is a major control, heat fluxes between the atmosphere and ocean are not perfectly analogous to those for CO_2. The difference is that the surface ocean-atmosphere equilibration time for CO_2 is finite (roughly 1 yr), [*Broecker et al.*, 1985]; for heat, the equilibration time is effectively infinite. To illustrate the difference between heat and CO_2, OCMIP includes an additional simulation where air-sea CO_2 fluxes are forced to be infinitely rapid.

We take the natural carbon cycle to be the state of the ocean-atmosphere carbon system prior to significant anthropogenic influence on the global carbon budget, usually considered to be the millenia leading up to the 19th century, when atmospheric CO_2 concentrations were "steady" at about 280 µatm.

The natural marine carbon cycle plays an important role in the partitioning of carbon dioxide between the atmosphere and the ocean through two important processes: the solubility pump and the biological pump [*Volk*, 1988], both of which act to create a global mean increase of dissolved inorganic carbon (DIC) with depth, and therefore to maintain atmospheric CO_2 at a level considerably lower by about a factor of three [*Najjar et al.*, 1992] than it would otherwise be.

The solubility pump maintains a vertical DIC gradient due to the fact that cold waters, which originate in high latitudes and fill up the deep ocean, can hold more DIC than warm waters at equilibrium with a fixed atmospheric pCO_2, a result of the higher solubility and dissociation of CO_2 (into carbonate and bicarbonate ions) in cold water. The vertical DIC gradient depends not only on the vertical temperature gradient but also the degree to which surface waters equilibrate with the atmosphere before sinking. Unlike most gases, the equilibration of surface water CO_2 with the atmosphere takes about one year, and therefore the strength of the solubility pump may depend critically on the kinetics of air-sea gas exchange.

The biological pump consists of two separate pumps: that of organic matter and calcium carbonate. The organic matter pump affects the DIC distribution through the photosynthetic formation of organic carbon in surface waters and the sinking and subsequent remineralization of this organic matter deeper in the water column. The carbonate pump affects the DIC distribution though the biogenic precipitation of calcium carbonate in surface waters and the subsequent sinking and dissolution of this material deeper in the water column. These two pumps also affect the alkalinity of seawater through the nitrate and dissolved calcium distributions.

Below, we present results from OCMIP equilibrium simulations designed to distinguish between these three effects: (a) the potential solubility pump which includes carbon chemistry, but wherein air-sea carbon fluxes are driven entirely by thermal fluxes [*Watson*, 1997] via forced (non-realistic) instantaneous equilibrium between pre-industrial air (278 ppmv) and surface waters (b) The biologic pump with its accounts for primary productions as well remineralization; we separately use a solubility pump which instead incorporates a finite (realistic) air-sea resistance to CO_2 gas exchange; and (c) the combined pump which include both the solubility and biological pumps. In addition, OCMIP separately added the anthropogenic component to the combined pump (the complete natural component) in order to compare the total of both to present-day measurements.

Resulting sea-to-air fluxes from the above experiments are displayed as zonal means for the Atlantic. The main patterns of sources and sinks of natural CO_2 are driven by the thermodynamics (i.e., heat fluxes). Thus all simulations exhibit out-gassing in the tropics and uptake in the high latitudes. However, potential fluxes are strongly attenuated by both the finite CO_2 gas exchange coefficient and by the biology . In reality, surface ocean CO_2 requires about a year to adjust to a CO_2 change in the atmosphere, so simulations show major differences where surface waters are replenished rapidly, i.e., in zones of upwelling and convection. Additionally, the biological pump counteracts the solubility pump either by bringing respired CO_2 (produced by bacterial degradation of organic matter) to the surface via upwelling and deep convection (in the high latitudes), or by consuming CO_2 at the surface via photosynthesis (in subtropical gyres and tropics). Validation of the natural carbon cycle is difficult because available data are scattered and polluted by anthropogenic CO_2. However, 1990 results from 3 OCMIP models exhibit roughly similar patterns as those observed in North-Atlantic by Takahashi et al. [*Takahashi and Sutherland*, 1995]. Anthropogenic fluxes in 1990 rival the magnitude of natural fluxes, especially in Austral ocean where the CO_2 sink has increased most since 200 yr ago.

With results from these same simulations, OCMIP investigated the north-south transport of carbon in the preindustrial ocean. All models suggest that there was not a large pre-industrial inter-hemispheric transport of CO_2. In contrast, based on an atmospheric model and atmospheric measurements of CO_2, Keeling et al. [*Keeling et al.*, 1995] extrapolated changes in the N-S gradient to infer that the preindustrial atmosphere transported roughly 1 Gt C yr-1 northward. They further reasoned that during preindustrial times, the global ocean should have transported an equivalent flux southward. All OCMIP simulations reveal a global-ocean carbon loop, transporting 0.6 Gt C yr-1 from Bering Strait,

across the Arctic Ocean, southwards through the Atlantic, across the Southern Ocean, and northwards again through the Indian and Pacific Oceans, back to Bering Strait. However, this loop is purely oceanic. It does not affect the inter-hemispheric budget for the atmosphere. Furthermore, air-sea gas exchange in the Northern Atlantic only weakly enhances the southward transport. If there were instantaneous equilibrium between air and sea (experiment a), southward carbon transport across the equator would increase by 50%, as expected by the large northward heat transport flux. However, all four experiments failed to produce the large disequilibrium between the North and the South as suggested by Keeling et al.[*Keeling et al.*, 1995].

INDIVIDUAL MODEL DESCRIPTIONS

Table 3 shows some of the important differences that exist between OCMIP models. With so many differences between the models themselves it is not easy to isolate the causes for discrepancies between even the most consistent simulations made as part of OCMIP. Although speculation is always possible as to why differences exist, the immediate focus of OCMIP is to determine where models differ and by how much.

Table 3: Some differences between OCMIP models.

Item	GFDL/Princeton	MPIM	IPSL	HADLEY
Model - Type	PE (MOM1)	LSG	PE (OPA7)	PE (Bryan/Cox)
Run	On-line	On-/Off-line	Off-line	On-line
Grid - Horizontal	96 x 40	72 x 72	180 x 15O	96 x 72
Vertical	12	22	30	20
Type	B	E	C	B
Rectangular	Yes	No	No	Yes
Forcing	Prognostic	Prognostic	"Semi-Diag."	Prognostic
Numerics (accuracy)	1st, 2nd	?	2nd	1st, 2nd
Free Surface	No	Yes	No	
Advection Scheme	Cent. Diff.	Upstream	FCT	Cent. Diff.
Seasonality	No	Yes	Yes	
Turbulence				
Vertical	Explicit	Numerical +Explicit	TKE (1.5 order)	KT-ML + Ri Explicit
Horizontal	1000-5000 m^2/s	Numerical	2000 m^2/s	80 m^2/s
Isopycnal Mixing	No	No	No	Redi/Cox
Gent and McWilliams	No	No	No	No

THE NEXT STEPS

Upcoming OCMIP efforts will investigate why models differ so much in the Southern Ocean, the most important sink for both natural and anthropogenic CO_2. A substantial effort will be mounted in order to better compare model results to available carbon system measurements, particularly (pCO_2, For such, models need to simulate both natural and anthropogenic components. Moreover, a proper understanding of the preindustrial carbon cycle is prerequisite to understanding changes that have and will take place. OCMIP will also begin to explore details of the relationships between CO_2 and two biogenic tracers: O_2 and C-13. Both now appear as promising tracers to help diagnose oceanic uptake of anthropogenic CO_2. Their relationships with CO_2 vary, however, between the different OCMIP models. Another facet of upcoming OCMIP efforts will be to take a more in-depth look at modelled ocean circulation fields, through the eyes of additional circulation tracers. Differences in model-predicted circulation fields are largely responsible for discrepancies between OCMIP simulations of the carbon cycle. OCMIP will validate simulated circulation fields by making runs for CFC's (inert transient tracers for which many oceanic measurements are now becoming available). Also, numerical

tracer simulations will be made as a means to better understand the role of the Southern Ocean in the global ocean carbon cycle.

The long range objective of OCMIP is to improve man's understanding of the ocean's carbon cycle and the crucial role of its major control--ocean circulation. Such critical information from ocean carbon-cycle models will be necessary to help governments and international organizations make informed decisions concerning future increases in atmospheric CO_2 and climate change. This understanding is also crucial to providing a firm base for proper evaluation of proposed geo-engineering solutions (e.g., ocean disposal of CO_2 as a means to help limit rising atmospheric CO_2).

Iron fertilization no longer appears a viable means to help sequester substantial amounts of anthropogenic CO_2, as shown by simulations with 3-D ocean carbon cycle models [*Sarmiento and Orr*, 1991]; [*Kurz and Maier-Reimer*, 1993]. Likewise, enhancing growth of marine macro-algae is not a reasonable option [*Orr and Sarmiento*, 1992]. On the other hand, ocean disposal of CO_2 as a means to artificially augment the ocean's transient uptake of CO_2 has not been thoroughly investigated. The only related global simulations have been made with an earlier version of the 3-D carbon cycle model from MPIM [*Bacastow and Stegen*, 1991]. The four OCMIP models differ substantially (e.g., regarding implementations of ocean turbulence and advection). Considering their resulting differences in the model output presented above, it is likely that they would also vary as concerns predictions related to ocean CO_2 disposal. It appears worth the effort to see just what the envelope of predictions might be.

NET PRIMARY PRODUCTIVITY MODEL INTERCOMPARISON ACTIVITY (NPP)

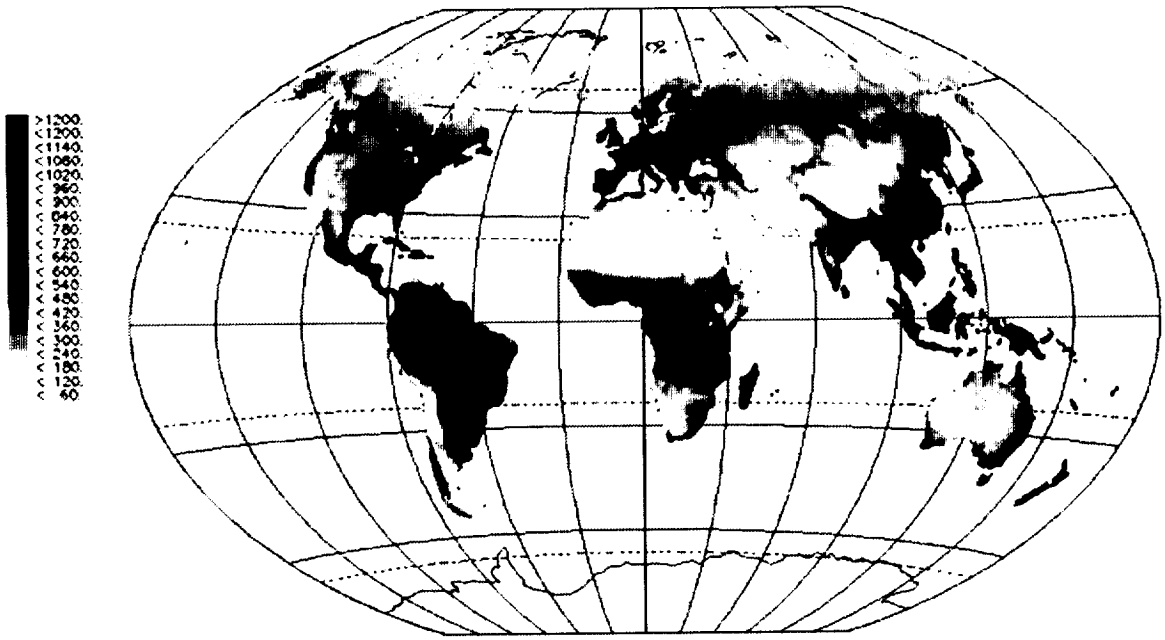

Global mean Net Primary Productivity, showing averaged results of 17 models compared at the 1995 NPP workshop in Potsdam, Germany.

OVERVIEW

Global Net Primary Productivity (NPP) of ecosystems on land and in the oceans is a crucial component of biogeochemical model development within IGBP. IGBP/GAIM, in conjunction with GCTE and IGBP-DIS has been investigating the performance of terrestrial ecosystem models which treat global NPP. This began with two model intercomparison workshops in 1994 and 1995 at the Potsdam Institute for Climate Impact Research (PIK). The purpose of the workshops was to support a series of model intercomparisons by the various designing teams around the globe that are currently modelling the terrestrial biosphere at large scales with a focus on NPP. The terrestrial carbon cycle models and models that treat energy and water fluxes must address in a fundamental manner either gross primary productivity (GPP) and/or net primary productivity (NPP).

There were significant differences in the calculation of NPP within the global terrestrial models compared in 1994, and Potsdam '95 was held in order to compare model parameters and outputs. Financial support for the workshops was provided by NASA, the European Commission, and the U.S. Environmental Protection Agency. Based on the results of model comparisons from the workshops, modelling teams returned to their codes to explore details of model performance. This has resulted in new insights regarding the terrestrial carbon cycle and the function of terrestrial ecosystems. On the basis of these new findings, several papers have been organized into a special issue of "Global Change Biology" featuring Net Primary Productivity, to be published in 1998. This GAIM report summarizes the results of the NPP model intercomparison activity in an attempt to set the stage for future refinement of terrestrial ecosystem models in the context of IGBP.

Future changes in global climate are anticipated as a consequence of the continuing rise in atmospheric CO_2. Predicted climate changes include an increase in mean annual air temperature and alterations in patterns of rainfall and cloud cover (Houghton et al., 1995). Understanding the response of vegetation to these changes is important because of dependence on plants for food, fuel and lumber. Vegetation also acts as a source, or sink, for the greenhouse gas CO_2. Net primary productivity (NPP), the net assimilation by plants of atmospheric CO_2 into organic matter, is driven by light and limited by unfavorable precipitation and temperature (Lieth 1975). Other factors such as nutrient availability and soil structure alter the ability of plants to fix carbon. Researchers have recently developed quasi-mechanistic simulation models of NPP. This was done in order to increase the predictive capacity of the regression based models.

As key components in the terrestrial carbon cycle, geographically referenced net primary productivity (NPP) and gross primary productivity (GPP) and their corresponding seasonal variations are needed to enhance understanding of both the functioning of living ecosystems and their effects on the environment. Productivity is also a key variable for the sustainability of human use of the biosphere through agriculture and forestry. Recently, it has become possible to investigate the magnitude and geographical distribution of these processes on a global scale by a combination of ecosystem process modelling and monitoring by remote sensing. Since agricultural and forestry production provide the principal food and fuel resources for the world, monitoring and modelling of biospheric primary production are important in order to support global economic and political policy making.

Sufficient data have only recently become available to properly characterize biosphere productivity. NPP is a quantitative characteristic of the biosphere and appears to be one of the most modeled ecosystem parameters at the global scale. From a theoretical viewpoint, NPP incorporates most of the annual carbon flux from the atmosphere to the biosphere and is considered to be the main cause of seasonal fluctuations in atmospheric CO_2 concentrations [*Ciais et al.*, 1995; *Keeling et al.*, 1996]. The practical importance of NPP estimation is found in its utility to measure crop yield, forest production and other economically and socially significant products of vegetation growth.

For estimates of the global carbon balance, a large amount of uncertainty centers on the role of terrestrial ecosystems. Geographically referenced GPP, NPP, heterotrophic respiration (R_h) and their corresponding seasonal variation are key components in the terrestrial carbon cycle. If we are to understand both the function of living ecosystems and their effects on the environment, then we must have a better grasp upon the controls and distribution of GPP, NPP, and R_H. This understanding of biological productivity is pivotal for sustainable human use of the biosphere. To understand the present and to predict the future role of ecosystems in this global context, observations are necessary, but insufficient, and a range of global terrestrial ecosystem models which capture the critical processes in the biosphere are needed. At least two factors govern the level of terrestrial carbon storage. First, and most obvious, is the anthropogenic alteration of the Earth's surface. An example of this is the conversion of forest to agriculture, which can result in a net release of CO_2 to the atmosphere. Second, and more subtle, are the possible changes in net ecosystem production (and hence carbon storage) resulting from changes in atmospheric CO_2, other global biogeochemical cycles, and/or the physical climate system. The significant influence of the terrestrial biosphere on the global carbon balance and hence on the problem of climate change has become more widely recognized during the past two decades[*Bolin et al.*, 1979; *Bolin et al.*, 1986; *Melillo et al.*, 1996; *Moore III et al.*, 1981; *Schimel*, 1995a; *Schimel*, 1995b]. Currently, the role of terrestrial ecosystems is recognized to be central to the residence time of carbon dioxide in the atmosphere [*Keeling et al.*, 1996; *Melillo et al.*, 1996; *Moore III and Braswell*, 1994].

In the last few years, a coordinated strategy has been developed to improve estimates of terrestrial net and gross primary productivity through measurement and modelling, mainly through the activities of the IGBP. The strategy has begun to yield dividends: several independent models now exist, others are in various stages of development, and it has become possible to investigate the magnitude and geographical distribution of primary productivity on a global scale by a combination of ecosystem process modelling and monitoring by remote sensing. These models range in complexity from fairly

simple regressions between key climatic variables and one or more estimates of biospheric trace gas fluxes to quasi-mechanistic models that attempt to simulate the biophysical and ecophysiological processes occurring at the plant level (including their scaling to large areas). Progress in model development has been significant in recent years, and this development has partly followed similar strategies in different groups. Each approach is based on simplifying assumptions about how ecosystems are structured and how vegetation may respond to changes in various environmental factors. Biospheric flux models all somehow (explicitly or implicitly) relate geographically specific and comprehensive estimates of temperature, water availability and photosynthetically active radiation (PAR), as well as their seasonal changes, to some or all of the basic processes of photosynthesis, growth and maintenance respiration, water and nitrogen fluxes, allocation of photosynthates in the plant and the production and decomposition of litter.

Among the models participating in the NPP intercomparison, two major groups can be distinguished based on the way they use various data sources. One group is essentially driven by observations made by space-borne sensors, most particularly the NOAA-AVHRR. This sensor now provides a relatively long time series and full global coverage with high temporal resolution. These models provide a steadily improved picture of the NPP of the world's actual vegetation. In contrast, most other models use data on climate and soils alone to derive estimates of the biological activity in the world's potential vegetation.

Table 1: Comparison of the broad features of the participating NPP models.

Model	Spatial resolution of NPP	Temporal resolution of NPP	NPP calculated as:	Influenced by[b]:	No. of VEGC pools
BIOME3	0.5° x 0.5°	1 month	GPP-R_A	GPP = f(SRad, LAI, Temp, AET/PET, CO_2) R_A = f(LAI, GPP)	0
BIOME-BGC	0.5° x 0.5°	1 day	GPP-R_A	GPP = f(SRad, LAI, Temp, SW, VPD, CO_2, LeafN) R_A= f(VegC, Temp)	4
CARAIB	0.5° x 0.5°	1 day	GPP-R_A	GPP = f(SRad, LAI, Temp, SW, VPD, CO_2, O_2) R_A = f(VegC, LAI, Temp)	2
CASA	1.0° x 1.0°	1 month	NPP	NPP = f(SRad, FPAR, Temp, AET/PET)	0
CENTURY	0.5° x 0.5°	1 month	NPP	NPP = f(VegC, Dead, Temp, SW, Prec, PET, N, P, S)	8
DOLY	0.5° x 0.5°	1 year	GPP-R_A	GPP = f(SRad, LAI, Temp, SW, VPD, CO_2, SoilC&N) R_A = f(VegC, T, SoilC&N)	2
FBM	0.5° x 0.5°	1 day	GPP-R_A	GPP = f(SRad, LAI, Temp, SW, CO_2) R_A = f(VegC, T)	2
GLO-PEM	8 km x 8 km	10 days	GPP-R_A	GPP = f(SRad, fPAR, Temp, SW, VPD) R_A = f(VegC, GPP)	2
HRBM	0.5° x 0.5°	1 month	NPP	NPP = f(Temp, Prec, AET/PET, CO_2, Fert)	0
HYBRID	0.5° x 0.5°	1 day	GPP-R_A	GPP = f(SRad, FPAR, Temp, SW, CO_2, N) R_A= f(VegC, Temp, VegN)	4
KGBM	1.0° x 1.0°	1 day	GPP-R_A	GPP = f(SRad, LAI, Temp, SW, VPD) R_A = f(GPP)	1
PLAI	0.5° x 0.5°	1 day	GPP-R_A	GPP = f(SRad, LAI, Temp, SW, CO_2) R_A= f(VegC, Temp)	2
SDBM	0.5° x 0.5°		NPP	NPP = f(SRad, FPAR, [CO2])	0
SIB2	4.0° x 5.0°	12 minutes	GPP-R_A	GPP = f(Srad, FPAR, LAI, Temp, SW, VPD, CO_2) R_A = f(GPP, Temp, SW)	2
SILVAN	0.5° x 0.5°	6 days	GPP-R_A	GPP = f(SRad, LAI, Temp, AET/PET, CO_2) R_A= f(VegC, Temp)	3
TEM	0.5° x 0.5°	1 month	GPP-R_A	GPP = f(SRad, KLeaf, Temp, AET/PET, CO_2, N) R_A = f(VegC, GPP, Temp)	1
TURC	1.0° x 1.0°	1 month	GPP-R_A	GPP = f(SRad, FPAR) R_A= f(VegC, Temp)	3

METHODS FOR THE COMPARISON

General considerations

At the Potsdam workshops, model comparisons were carried out by a combination of standardized model runs (including common visualization methods), group discussions among the modeling teams

to understand the conceptual differences among the models and subsequent analyses by working groups. Absolute standardization of all external data sets, spatial scale assumptions etc. is not achievable for a broad comparison of this type. Some models are designed to operate with different data sets than others, for example—forcing them to using a standard input file would therefore yield misleading results. We aimed, however, for the highest possible level of standardization, using i) a common spatial framework and input data sets, and ii) a common visualization toolbox.

Common data sets

Being climate-driven, all NPP models have requirements for data on *temperature* and *moisture availability*. With the exception of GLO-PEM (spatial resolution 8 km x 8 km) and SIB2 (4.0° x 5.0°), the models already used climate data sets that were gridded at 0.5° longitude/latitude resolution (approx. 55 km at the equator, but shorter in longitudinal direction towards the poles)—some others were run at that resolution to allow direct comparison at the workshop. Again, apart from GLO-PEM and SIB2, the models operate with monthly long term means of climate. Those running at daily time steps usually generate quasi-daily climate data from monthly averages internally. A few models interpolate quasi-hourly climate data for estimating GPP whereas others (e.g., CARAIB, HYBRID) applied weather generators [*Friend*, in press; *Hubert et al.*, in press] to simulate daily variability. With the same exceptions, the models used the same land sea mask which results from selecting all land areas except Antarctica and counting the cells from a global 0.5° grid (62483 cells). For this land mask, the CLIMATE data base (long term mean 1931-1960, version 2.1, [*Cramer et al.*, in prep; *Leemans and Cramer*, 1991] was provided to the participants for monthly mean temperatures and precipitation values.

Solar radiation is required by most models, but the formulations for estimating it differ among the models. Those models that estimate radiation from location (latitude) and cloudiness used a gridded estimate of the number of sunshine hour percentages (as a proxy for cloudiness) from the same CLIMATE data base [*Otto et al.*, manuscript]. SIB2 is intimately linked with the Colorado State University general circulation model (CSU-GCM), which has a rather coarse spatial resolution (4° latitude x 5° longitude), and a high temporal resolution (hourly or less). SIB2 develops its NPP estimates at that spatial and temporal resolution.

With the same objective of simplifying the model comparisons, it was suggested that those models that require satellite data for the quantitative prescription of *seasonal changes in FPAR* use the same data product from the global records of the Advanced Very High Resolution Radiometer (AVHRR): the FASIR data set for 1987 of the ISLSCP CD-ROM database [*Meeson et al.*, 1995; *Sellers et al.*, 1994]. This data set consists of monthly NDVI at a spatial resolution of 1° with improved processing compared to the standard GVI product widely used before. The seasonal FPAR required by the satellite-based models is derived from this FASIR-NDVI. However not all satellite-based models were developed using the FASIR data set, and their adaptation to it produced deteriorated results for the comparison. A fundamental problem is that some models are conceptually developed for different satellite data sets. GLO-PEM, for example, was designed to use satellite data at a higher temporal and spatial resolution (AVHRR Pathfinder) which also provide other information (e.g. surface temperature, humidity) that are not available from the FASIR data set. Therefore, the results of GLO-PEM analyzed at the Potsdam'95 workshop are neither the optimal nor do they correspond to the published values because the use of the FASIR data set to describe other satellite-derived variables. The results of TURC are also non optimal, and different from the published ones, because it was not possible to adjust some relationships for the use of the FASIR data in time for the workshop. Only CASA and SIB2 are designed for the FASIR data set. The results available for SDBM are those of the Potsdam'94 workshop, using another satellite data set. Therefore the outputs of SDBM have generally not been considered in the intercomparison results, apart from in the papers about light interception/light use efficiency and seasonality. Future intercomparisons need to be aware of the fact that standardization of data sets may also create these types of artifacts.

In addition, the satellite data used correspond generally to observations of the specific year 1987, while the input climate data used are the 1931-1960 long term means at the exception of GLO-PEM and SIB2. The years from 1931-1960 years may be considered anomalous in parts of the tropics [*Hulme*, 1992]. The effect of this inconsistency on global NPP is probably limited, but the diagnostic values given to those models combining non-contemporary satellite derived vegetation activity and climate (although highly useful) must be treated cautiously.

Among the data sets that could *not* be standardized for the intercomparison were *average humidity* and *wind speed*, which were required by some models. *Vegetation distribution* is an input to several models, and the selected maps (or models) affect results both at the levels of model calibration and application. This feature is central to most models—a strict standardization could have removed features that are critical for the individual model design. Furthermore, the models that estimate both fluxes and vegetation structure (BIOME3, DOLY, HYBRID) do not predict identical vegetation distributions. Practically all *soils* data came from the FAO Soil Map of the World (FAO/UNESCO 1974), but the interpretations of its categories in terms of soil factors were not standardized across models. Some models have used the translation of the Zobler soil texture (1986) to field capacity and wilting point. Pan *et al.* (1996) have recently shown the uncertainty of biosphere models to such different soil data sets.

RESULTS

Total annual net primary production

The models estimate the net primary production of the terrestrial biosphere to be between 39.9 and 80.5 Pg C yr^{-1} with a mean of 54.9 Pg C yr^{-1}. Table 2 shows the estimated global NPP values for each model in decreasing order. Although much effort has been paid to reduce the variability among modelled NPP estimates through the use of common data sets, these global NPP estimates are still based on different land areas used by the models (Table 5). The area of the terrestrial biosphere varies from 105.6 to 128.7 10^6 km^2. This variability is about 18 percent of the 128.7 10^6 km^2 represented by the 56,785 grid cells of the common input data sets. The variation is caused partly by i) missing data—some models do not estimate NPP for some vegetation classes (e.g., FBM does not estimate NPP for desert regions; TEM does not estimate NPP for wetland or floodplain vegetation types); ii) the use of additional data sets that do not exactly match the grid cells used in the common data sets; and iii) for SIB2, the coarse spatial resolution used to calculate NPP. These differences do not appear to have a major influence on global NPP estimates because they are partially compensated by other differences, or because they concern the missing regions which have relatively low productivity.

Table 2: Comparison of annual and monthly NPP of the globe and the factors influencing NPP among sixteen models, ranked in decreasing order of global annual NPP estimates.

Model	NPP ($Pg\ C\ yr^{-1}$)	Number of grid cells	Area ($10^6\ km^2$)	Mean length of growing season[a] (months)	Monthly maximum global NPP ($Pg\ C\ mo^{-1}$)	Monthly minimum global NPP ($Pg\ C\ mo^{-1}$)	Seasonal range in global NPP ($Pg\ C\ mo^{-1}$)	Temporal resolution of NPP	Veg[b]	NDVI	Moisture[c]	Nutrient Constraints[d]
TURC	80.5	56785	128.7	10.5	9.1	4.8	4.3	monthly	A	FPAR		
GLO-PEM	66.3	56785	128.7	6.0	7.7	3.4	4.3	monthly	A	FPAR and others	SW/VPD	
CARAIB	65.2	56785	128.7	6.3	8.4	3.8	4.6	daily	A(M)		SW, VPD	
KGBM	62.5	56785	128.7	6.4	9.1	2.8	6.3	daily	P(D)	PHENO	SW, VPD	
BIOME-BGC	62.2	54279	124.0	6.2	8.4	2.9	5.5	daily	P(D)		SW, VPD	Leaf-N
SILVAN	61.1	56785	128.7	6.8	7.7	3.5	4.2	6days	P(D)		AET/PET	
BIOME3	54.2	56785	128.7	7.5	6.6	3.0	3.6	monthly	P(M)		AET/PET	
CENTURY	53.3	50641	116.9	8.3	6.2	2.9	3.3	monthly	P(B)		SW, Prec	N, P, S
FBM	49.9	47807	105.6	7.4	7.5	2.5	5.0	daily	P(B)		SW	
PLAI	49.2	56785	128.7	5.2	6.6	2.0	4.6	daily	P(B)		SW	
CASA	48.9	56785	128.7	9.1	5.8	3.1	2.7	monthly	A(D)	FPAR	AET/PET	
SIB2	47.9	51050	115.7	7.1	8.3	2.2	6.1	12mn	A(D)	FPAR and others	SW, VPD	
DOLY	46.4	56785	128.7	N/A[e]	N/A	N/A	N/A	year	P(D)		SW, VPD	Soil C&N
TEM	46.2	55290	125.6	6.8	6.7	2.4	4.3	monthly	P(B)		AET/PET	N
HRBM	44.3	56785	128.7	6.0	5.6	2.3	3.3	monthly			Prec, AET/PET	Fert
HYBRID	39.9	56785	128.7	5.7	7.0	-1.6	8.6	daily	P(M)		SW	Veg-N, N

a A specific month is considered part of the growing season if its NPP estimate is greater than 10% of the maximum monthly NPP estimate of the grid cell.

b NPP estimates are based on the assumption that the world is either covered with potential (P) or actual (A) vegetation. Vegetation type may be either an input variable; implicit within the model (e.g. NDVI data only represents actual vegetation); or explicitly simulated by the model. Within a grid cell, the vegetation may be assumed to be represented by a single dominant (D) vegetation type or a mosaic of vegetation case. In the latter case, the model considers either an average parameterization that is biome-dependent (B), or a distinct parameterization for each vegetation type (M).

c The effect of soil moisture on NPP may be described either by using precipitation (Prec), soil water (i.e. soil moisture, soil water potential - SW), vapor pressure deficit (VPD), or actual evapotranspiration (AET) and potential evapotranspiration (PET)

d Nutrient constraints may be implemented based on a soil fertility factor (Fert), on the carbon and nitrogen content of soil organic matter (Soil C&N), on the nitrogen content of leaves (Leaf-N), the nitrogen content of both leaves and roots (Veg-N), and/or on inorganic nitrogen (N), phosphorus (P), or sulfur (S) concentrations in the soil.

e N/A is not applicable because DOLY estimates only annual NPP

(Haxeltine & Prentice 1996) (Haxeltine *et al.* 1996) (Running & Hunt 1993) (Warnant *et al.* 1994) (Nemry *et al.* 1996) (Potter *et al.* 1993) (Field *et al.* 1995) (Parton *et al.* 1993) (Woodward *et al.* 1995) (Kindermann *et al.* 1993) (Lüdeke *et al.* 1994) (Kohlmaier *et al.* 1997) (Prince 1991) (Prince & Goward 1995) (Esser *et al.* 1994) (Friend & Cox 1995) (Friend *et al.* 1997) (Kergoat in press) (Plöchl & Cramer 1995b) (Plöchl & Cramer 1995a) (Knorr & Heimann 1995) (Sellers *et al.* 1996b) (Sellers *et al.* 1996a) (Randall *et al.* 1996) (Kaduk & Heimann 1996) (McGuire *et al.* 1995) (McGuire *et al.* in press) (Ruimy *et al.* 1996)

The two extreme global NPP values estimated by TURC and HYBRID have specific explanations. The TURC simulations for Potsdam'95 were made with the FASIR data set without appropriate re-calibration, which results in an overestimation of the NPP fluxes compared to other published results: 62.3 Pg C yr^{-1} for the reference computation and 71.3 Pg C yr^{-1} when the FASIR data set is used with re-calibration [*Ruimy et al.*, 1996]. The use of FASIR without re-calibration also causes the growing season to become unrealistically long. The low global NPP for HYBRID may be explained by the fact that HYBRID considers a pre-industrial atmospheric [CO_2] of 280 ppmv (Andrew Friend, pers. comm.) whereas the other models consider atmospheric [CO_2] concentrations to be between 340 and 360 ppmv (Table 4).

If TURC and HYBRID are left aside, then the range of variation of the global NPP results is reduced from 100% to 50%, which must be considered to be a relatively good agreement for the estimation of this poorly understood variable. The explicit calibration procedures used by some models are certainly partly responsible for this, and the results of Ruimy *et al.* suggest that most NPP models may indeed be calibrated so that annual global NPP are within 'commonly admitted values'.

Table 2 shows that the overall ranking of global NPP cannot be explained by any of the specific model features described below, and certainly not by the basic categories of Table 3. Satellite-based models may estimate high values of global NPP (GLO-PEM, TURC), but they also estimate low values (CASA, SIB2). The three models which do not require GPP estimation (CASA, CENTURY, HRBM) display intermediate to low values. It must be noticed, however, that four of the six models which apply nutrient constraints on NPP estimate lower global NPP than models not considering nutrient constraints.

Four of the six models which used vapor pressure deficit to determine NPP estimate higher global NPP than those using other approaches to describe the influence of moisture on NPP. This result shows that NPP estimates may be sensitive to the modeling strategy used to simulate the water balance and the effect of water stress on NPP. One of the models using vapor pressure deficit that predicted a lower global NPP (DOLY) also implemented nutrient constraints on NPP.

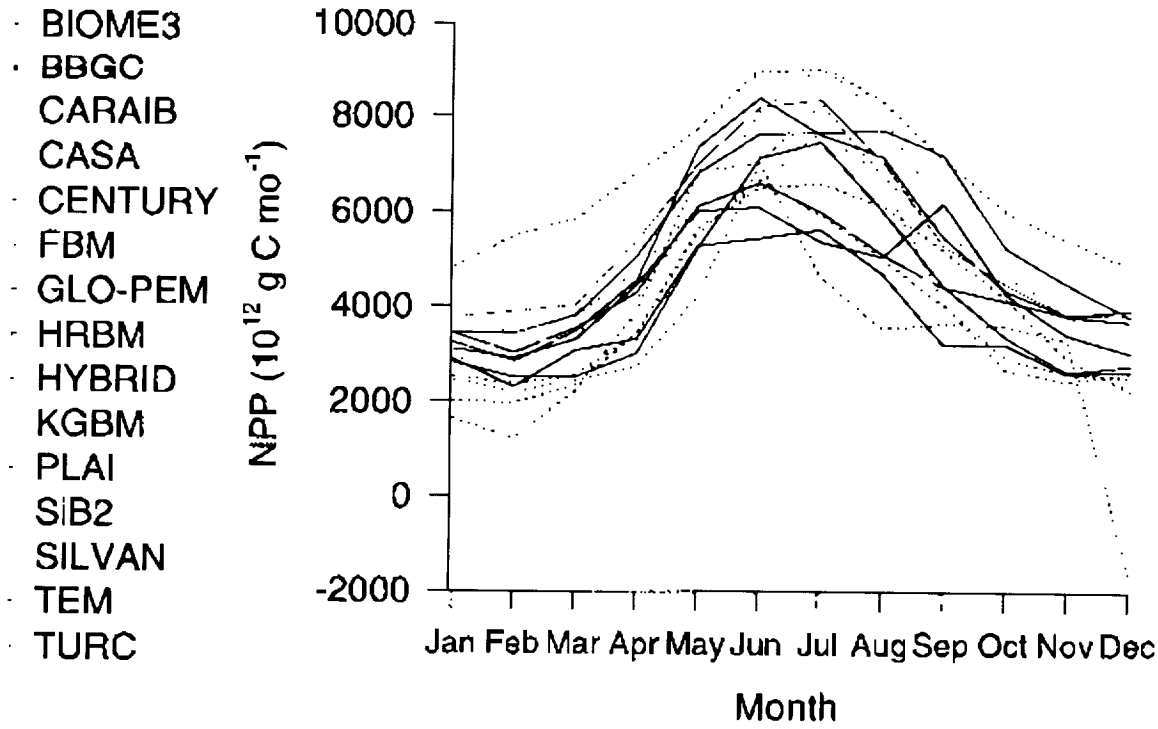

Figure 1
Comparison of seasonal variations in global net primary production among models.

Most models estimate the lowest NPP to occur in February (CARAIB, CASA, TURC in January, HYBRID in December). The lowest monthly global NPP ranges from -1.6 Pg C mo^{-1} (HYBRID) to 4.8 Pg C mo^{-1} (TURC), the extremes being the same, partly for the same reasons as for the global values. A negative NPP indicates that plant respiration is greater than the uptake of carbon by plants during a month when vegetation is stressed by drought conditions or low temperatures. All models estimate that the highest monthly global NPP occurs during the northern summer, apart from CENTURY which estimates the peak to occur in September due to a particular artifact (W. Parton, pers. comm.). The highest monthly global NPP ranges from 5.6 Pg C mo^{-1} (HRBM) to 9.1 Pg C mo^{-1} (KGBM and TURC).

The seasonal range in monthly estimates of global NPP differs among models (Table 5). The seasonal variations of HYBRID in global NPP (8.6 Pg C mo^{-1}) are more than three times larger than the seasonal variations of CASA (2.7 Pg C mo^{-1}). The table shows that the intensity of the growing season is stronger in the daily models than in the monthly models. Models that use vapor pressure deficit (VPD) or soil moisture (SW) also estimate higher seasonal ranges in global NPP than approaches that use monthly precipitation (Prec), AET or PET. Many of the 'daily' models use variations of the Penman-Monteith algorithm to describe the influence of moisture on NPP. It appears as if the use of different algorithms to describe the effect of moisture on NPP by the various models affects the amplitude of the seasonal variations. The daily canopy models also display a rather strong NPP seasonality. Seasonal NPP, LAI, and FPAR profiles, annual NPP and vegetation characterisation along an American transect from North (58.5°N, 63.5°W) to South (31 °N, 84 °W) are shown in figure 2. The seasonal NPP, LAI, FPAR profiles along an African transect from North (17.5 °N, 12.0 °E) to South (0 °N, 12.0 °E) are shown in Figure 3.

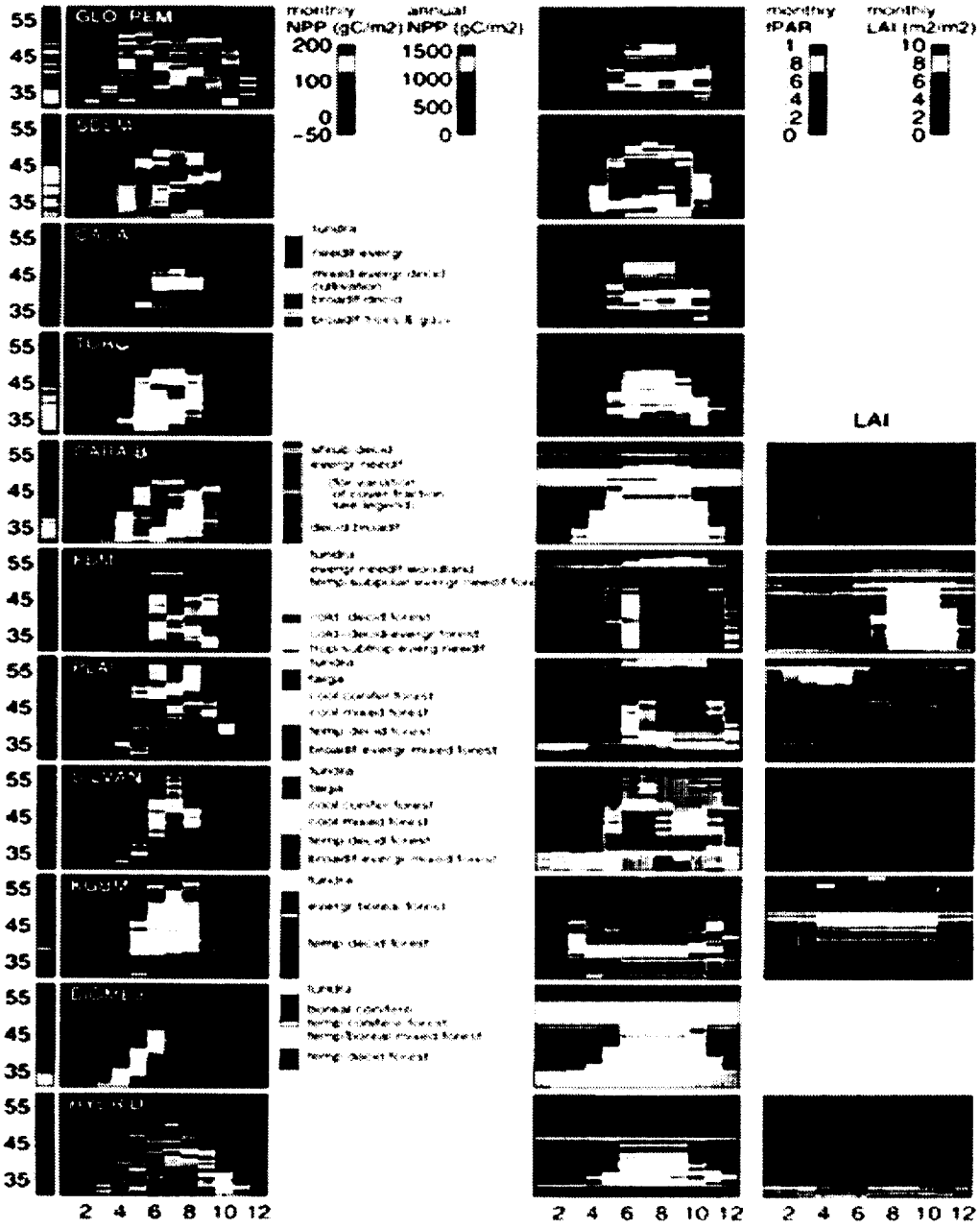

Figure 2: Phase diagrams of the monthly NPP, FPAR and LAI (only for the canopy models) along the north-south transect (radiation and temperature gradient) over eastern North America: (58.5 °N, 63.5 °W) to (31 °N, 84 °W). The order of the models is the same as before. The horizontal axis denotes the 12 months, the vertical the latitudes. For each model, the annual NPP along that transect is indicated on the left side of the phase diagram of monthly NPP, and an indication of the vegetation structure associated with each grid cell, is indicated on the right side when the model employs one, either as input, or as output (BIOME3). For CARAIB, only the forest type is indicated, but the model works with cover fraction of different PFTs within each grid cell: forest cover fraction increases regularly from the north to the boundary between evergreen and deciduous (from 10% to 80%), while C_3 grass cover fraction decreases in the same direction (from 50% to 20%). Then deciduous broadleaf forests and C_3 plants (grasses + crops) share the southern part.

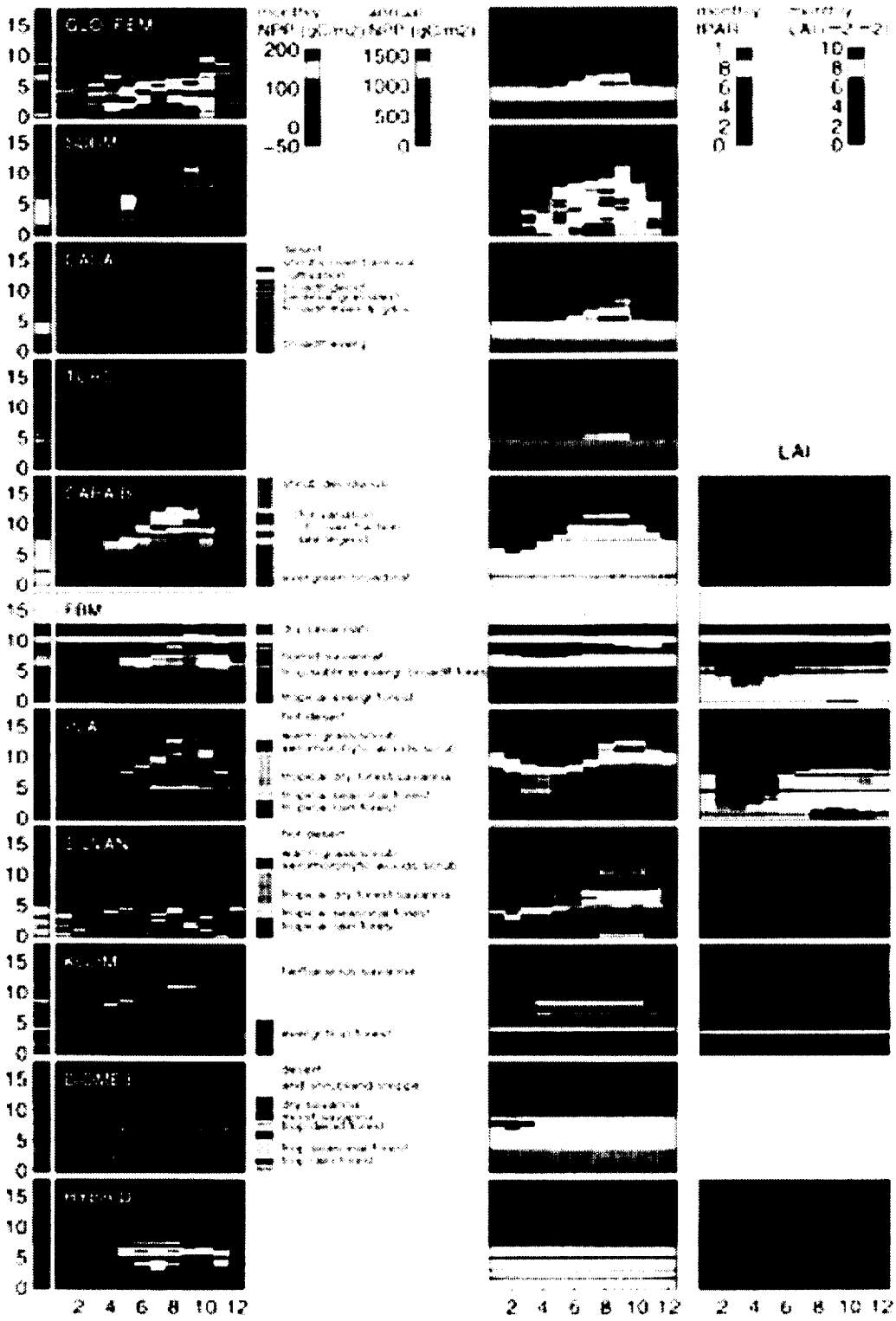

Figure 3. The same as Fig. 3 for the north-south transect (precipitation gradient) in Africa (17.5 °N, 12 °E) to (0 °N, 12 °E). For CARAIB, the southern end of the transect has a maximum forest cover fraction (80-100%), the middle part has C_3 grasses and crops (around 40%), C_4 grasses and crops (around 20%) and forest (around 10%), and the northern part only a 10% cover of C_4 grasses.

Differentiation of NPP by major biomes

Comparison of the Latitudinal Distribution of Net Primary Production among Models

The relatively fine spatial resolution (0.5° longitude/latitude) of the NPP estimates provided by the various groups for the Potsdam workshops allows model intercomparisons at many spatial scales. Kicklighter *et al.* (this issue) compare the latitudinal distributions of annual and seasonal NPP estimates among the models and how estimates of NPP for various biomes may influence these latitudinal distributions of NPP. We find that most models estimate a bimodal distribution of annual NPP across the globe with the highest production occurring around the equator and a second smaller peak in production occurring between 50° and 60° N. Although the large land area between 50° and 60° N accounts, in part, for the second NPP peak, both of these regions along with a third latitudinal band in the southern hemisphere (35° to 45° S) represent regions with high rates of productivity per unit of area. These three latitudinal bands are also the regions with the highest variability in NPP estimates among the models. The variability in NPP estimates appears to be related to differences in simulating the effects of moisture on NPP in the tropical latitudinal band and differences in simulating the effects of nutrient constraints on NPP in the southern temperate latitudinal band. In the northern temperate/boreal latitudinal band, variability in NPP estimates is related to both these factors along with differences in simulating the capture and use of solar radiation. The tropical latitudinal band appears to be dominated by tropical evergreen forest and the northern temperate/boreal latitudinal band appears to be dominated by boreal forests. No biome appears to be predominant in the southern temperate latitudinal band.

Although NPP is seasonal in tropical and subtropical regions, seasonal variations of global NPP appear to be mostly influenced by seasonal NPP in boreal regions. Most models estimate higher NPP in boreal forests than in tropical evergreen forests during June, July and August as a result, in part, of the longer day lengths experienced by boreal forests during the summer in the northern hemisphere.

Within these general trends, the latitudinal distribution of NPP varies considerably among the models. Although the latitudinal distribution of NPP is useful for describing the influence of the terrestrial biosphere on atmospheric CO_2 dynamics, it is not as useful for model comparisons because the differences among the models are confounded with latitudinal variations in land mass. To eliminate this bias, we compared the area-weighted mean NPP (i.e., areal NPP) of latitudinal bands among the models. As a result of this normalization: 1) the relative size of the peak in primary production found in the northern hemisphere is much reduced; 2) a third peak in primary production appears between 45 and 35° S; 3) the tropical peak in primary production has shifted to exist between 5° S and 5° N; and 4) the relative differences between the models become larger. In addition, a small peak in areal NPP estimated by FBM occurs in the latitudinal band between 15 to 25° N. As FBM does not provide NPP estimates for desert regions, it's areal NPP estimates are based on fewer, more productive grid cells than the other models. The latitudinal distribution of areal NPP is very similar to the latitudinal distribution of precipitation indicating the importance of moisture on the NPP estimates of all the models. The high primary production in the tropics and the 45 to 35° S latitudinal band is probably also associated with the higher temperatures (Figure 4) and solar radiation (Figure 4) found in these regions, but the relationship of the latitudinal distribution of NPP to these climatic variables is not as clear as the influence of precipitation.

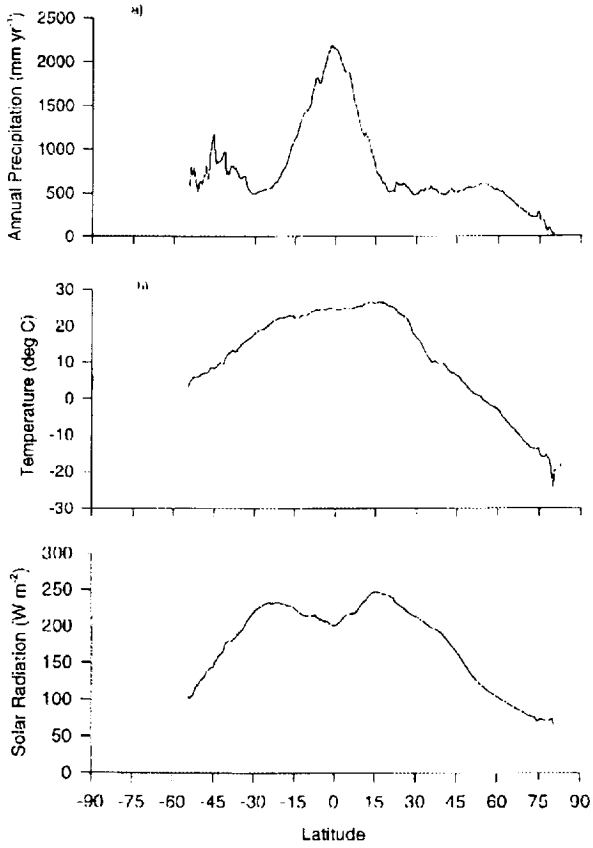

Figure 4. Latitudinal distribution of (a) annual precipitation; (b) mean annual air temperature (^{o}C); and (c) mean annual solar radiation. All values represent area-weighted means for the land mass located within a 0.5^{o} latitudinal band.

Similar to the latitudinal distribution of areal NPP, the latitudinal distributions of mean growing season lengths (Figure 5) of most models are trimodal. All models have long growing seasons (10 to 12 months) near the equator. In addition, a second peak in mean growing season length occurs between 50 and 30° S with some models again estimating a growing season that lasts almost year-round. The mean growing season generally decreases for all models from the equator to the north pole, although large differences exist in the latitudinal patterns of this trend among the models. As mean annual temperature and solar radiation also decrease from the equator to the poles (Figure 4b and 4c), the latitudinal pattern of the growing season lengths reflect the importance of these climatic variables on NPP estimates for all the models. With the exception of the CASA and TURC models, most models estimate a third peak in mean growing season length in the northern hemisphere, but the location of this peak varies among models from 20 to 50° N.

Unlike the other two peaks, the long growing season in the northern hemisphere is not associated with a peak in areal NPP which occurs in the latitudinal bands between 50° and 60° N in most models. This result suggests that variations in the intensity of NPP during the growing season have a larger influence on annual NPP estimates of most models in the northern hemisphere influence than growing season length. In contrast, the areal NPP estimates of the CARAIB, GLO-PEM and PLAI models do appear to be related to growing season length in the northern hemisphere. In addition, the longest mean growing season in the northern hemisphere is only six to nine months compared to the nearly year-round growing season of some models in the southern hemisphere. Thus, the temperate regions of the southern hemisphere have a longer mean growing season than comparable latitudes of the northern hemisphere, although there is considerable variability among the models. The longer growing season of the temperate regions of the southern hemisphere (35 to 45° S) may be a result of the warmer

(+4.3^{o} C) and wetter (+300 mm yr^{-1}) climate than that found at comparable latitudes of the northern hemisphere even though the amount of solar radiation is about the same (Figure 4).

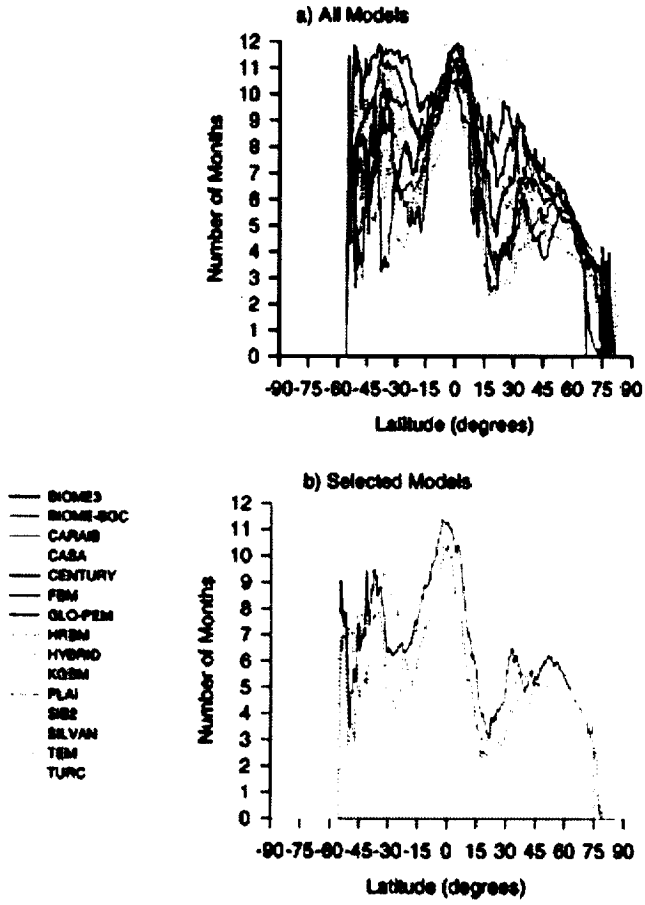

Figure 5. Comparison of the latitudinal distribution of mean growing season length: (a) among all models; and (b) among the CARAIB, CASA, HYBRID and PLAI models. All values represent area-weighted means for the land mass located within a 0.5° latitudinal band.

The CASA and TURC models have a similar latitudinal distribution of growing season lengths that is very different from the other models. Both models estimate very long growing seasons for a latitudinal band between 45° S and 25° N. The long growing season estimated by TURC extends even further to about 40° N. Although the long growing season is partly responsible for the high NPP estimated by TURC across the globe, the latitudinal NPP estimates by CASA do not appear to be influenced by growing season length. This long growing season is partly explained by the fact that these models are strongly constrained by the seasonality of the FASIR-NDVI data set which shows a rather smoothed seasonality and assumes no seasonality at all for some vegetation types. The light use efficiency for gross primary production in TURC is constant over the whole globe so that the latitudinal variability in NPP is caused only by latitudinal variations in solar radiation and respiration costs linked to temperature. Therefore, the length of the growing season partly drives the latitudinal distribution of NPP in TURC. In contrast, local environmental factors reduce the light use efficiency in CASA so that the length of the growing season does not have such a large influence on the latitudinal distribution of NPP in CASA.

Comparison of Net Primary Production of Biomes among Models

With the exception of BIOME-BGC, all models estimate that the grid cells grouped as tropical evergreen forests in this study have the highest mean biome NPP among the biomes (Figure 6a). For TURC, these results are not consistent with the results of Ruimy *et al.* (1996a) where the model estimated the highest NPP occurred in tropical savannas. The difference in the results of these two studies may be related to the use of different vegetation data sets and different vegetation classification schemes. Most models also estimate that temperate broadleaved evergreen forests are the next productive biome. With the exception of BIOME3, FBM, and TURC, arid shrublands/deserts are the least productive biomes among the models. Most models also estimate that tundra and boreal woodland have low productivity. Besides these biomes, the relative order of mean biome NPP varies among models. The ranking of mean biome NPP for tropical savannas varies the most among the models. The SIB2 model estimates tropical savannas to be the second most productive biome whereas the GLO-PEM model estimates tropical savannas to be the tenth most productive biome of the fourteen biomes identified in this study. Generally, mean biome NPP increases from cold, dry biomes to warm, moist biomes (Figure 6a). In corresponding latitudinal zones (i.e., boreal, temperate, and tropical), forests have higher mean biome NPP than savannas, grasslands, or shrublands for most models. Interestingly, most models estimate that the grid cells grouped as grasslands in this study have a higher mean biome NPP than grid cells grouped as temperate savannas. The greatest range in mean biome NPP among the models occurs in the productive temperate broadleaved evergreen forests, but considerable variability among mean biome NPP estimates (as indicated by the large intervals between the 25th and 75th percentiles shown in Figure 6a, also occurs in temperate mixed forests, temperate deciduous forests, and boreal forests. Mean biome NPP estimates for tundra have the smallest range, but mean biome NPP estimates appear to be the most similar for arid shrublands/deserts. In general, the variability of mean biome NPP estimates among the models increases with the magnitude of the mean biome NPP estimates.

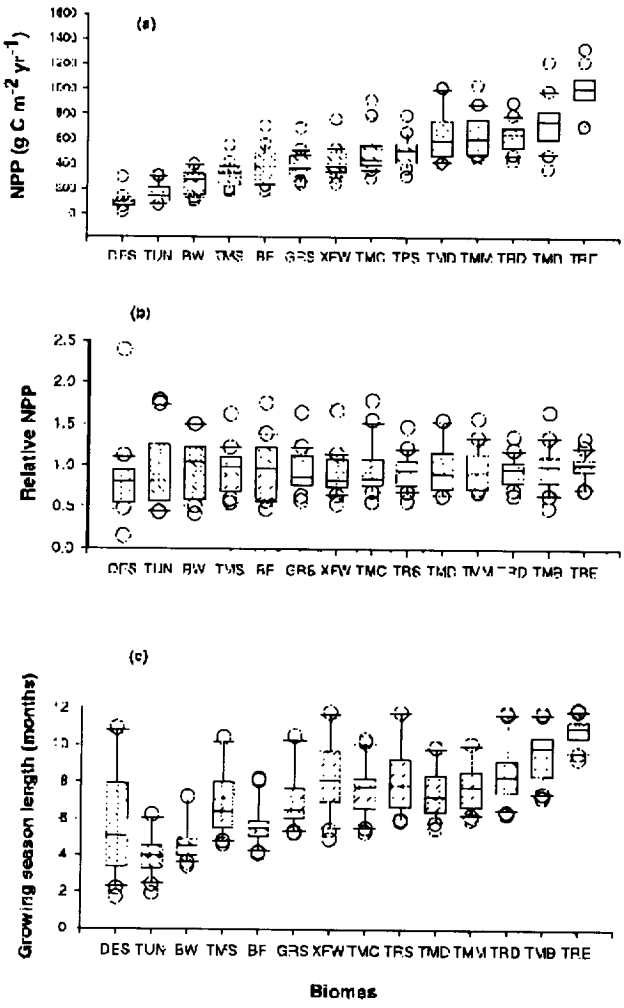

Fig 6. Comparison among biomes of the variability in model estimates for (a) mean biome net primary production; (b) mean biome net primary production relative to that estimated from the combined model results (i.e., grid cell NPP estimated as the average of all model NPP estimates); and (c) mean growing season length within a biome. Biomes include arid shrublands/deserts (DES), tundra (TUN), boreal woodlands (BW), temperate savannas (TMS), boreal forest (BF), grasslands (GRS), xeromorphic woodlands (XFW), temperate conifer forests (TMC), tropical savannas (TRS), temperate deciduous forests (TMD), temperate mixed forests (TMM), tropical deciduous forests (TRD), temperate broadleaved evergreen forests (TMB) and tropical evergreen forests (TRE). Biomes are arranged in ascending order of the mean biome NPP estimated from the combined model results. Bars within the boxes represent median values. The bottom and top of the box represents the 25th and 75th percentile, respectively. The bars outside the box represent the 10th and 90th percentiles. Open circles represent outliers.

Although the absolute differences in mean biome NPP estimates appear to be small in arid shrublands/deserts, the largest relative differences in mean biome NPP among the models occur in this biome (Figure 6b). The mean biome NPP estimate of TURC (296.2 g C m^{-2} yr^{-1}) is almost sixteen times the mean biome NPP estimate of DOLY (18.7 g C m^{-2} yr^{-1}). The TURC model does not consider the effect of water limitation on GPP, other than that resulting from a diminished NDVI. As light use efficiency for GPP is constant, higher NPP occurs in areas experiencing water stress. However, TURC may also overestimate NPP in shrublands because a non-appropriate calibration was used to derive FPAR from the NDVI data (A. Ruimy, personal communication). Generally, the uncertainty in the mean biome NPP estimates of the biomes in the boreal region (i.e., tundra, boreal woodlands, boreal forests) are greater (as indicated by the large intervals between the 25th and 75th percentiles in Figure 6b) than the uncertainty in other biomes. Tropical evergreen forests have the smallest relative differences in mean biome NPP estimates. The mean biome NPP estimate of CENTURY (1333.7 g C m^{-2} yr^{-1}) is less than twice that of HRBM (709.3 g C m^{-2} yr^{-1}) in tropical evergreen forests.

Similar to the mean biome NPP estimates, the models generally show longer mean growing seasons from cold, dry biomes to warm, moist biomes (Figure 6c). Tundra has the shortest growing season and

tropical evergreen forests have the longest growing season. Dry biomes have considerable variability in mean growing season lengths with the greatest range of growing season lengths occurring in arid shrublands/deserts. The mean growing season length estimated for arid shrublands/deserts by the TURC model (10.9 months) is 9.2 months longer than that estimated by the PLAI model (1.7 months). In contrast, the mean growing season lengths are the most similar for tropical evergreen forests. Both the CASA and TURC models estimate a mean growing season length (11.8 months) that is only 2.5 months longer than that of the PLAI model (9.3 months). As mean growing season lengths correlated (i.e., Spearman's coefficient of rank correlation; $p < 0.05$) to mean biome NPP in arid shrublands/deserts, boreal forests, temperate mixed forests, temperate deciduous forests and tropical deciduous forests, differences in mean NPP estimates among the models for these ecosystems are related to differences in the length of the growing season assumed by the various models.

The ranking of the models for the mean biome NPP estimates of tropical evergreen forests is similar to the ranking for areal NPP estimates within the tropical latitudinal band (i.e., 5° S to 5° N). In addition, the ranking of the models for the mean biome NPP estimates of boreal forests is similar to the ranking for areal NPP estimates within the northern temperate/boreal latitudinal band (i.e., 50° N to 60° N). An examination of the latitudinal distribution of the fourteen biomes indicates that these biomes are indeed predominate in these particular latitudinal bands. Thus, the magnitude and variability of NPP estimates in tropical evergreen forests and boreal forests have a large influence on the magnitude and variability of global NPP estimates. As a result, an examination of the seasonal patterns of NPP in these two biomes may provide insights into the factors controlling the seasonal patterns of global NPP.

CONCLUSIONS

This first systematic comparison of terrestrial biogeochemical models, using what appears to be its most significant flux variable (NPP), has shown agreement between the present generation of models for many broad features of the overall behavior, despite the fact that the models had been developed for widely differing purposes and with widely differing resource bases for personnel and computing power. However, and perhaps more interestingly, both the differences in model behavior and the unresolved question of calibration to an assumed total NPP have identified important shortcomings in our understanding of the total Earth system. These need to be reduced if predictions or sensitivity assessments of the stability and sustainability of the terrestrial biosphere, are demanded. Better predictivity cannot come from improved physical models of the ocean and the atmosphere alone, even if these too are needed. Most recent assessments of the future of the coupled system [*Melillo et al.*, 1996] have highlighted that it is likely to be highly sensitive to the dynamics of the biosphere as well.

Recently, new technological and scientific developments have indicated that our ability to observe changes in biospheric activity may be greater than anticipated: Keeling *et al.* (1996) made the convincing point that, at least over the period since 1960, biospheric activity in northern latitudes may have changed strongly enough to produce an average extension of the growing period by seven days, and Myneni *et al.* (1997) used the AVHRR satellite record to confirm this result, while also indicating the regional uncertainties. The modelling teams aiming at simulating global carbon fluxes now face the challenge to explain or reject these and other hypotheses about the dynamics of the Earth's vegetation.

To meet this challenge, several activities are now underway—some of them being spawned off from the NPP workshops:

• Numerous 'minor findings' from the working group discussions have already lead to improved versions of the various models. In several cases, only the thorough scrutiny provided by colleagues during the comparison process could identify errors or minor inadequacies that subsequently have been removed from the models.

• The importance of an improved data basis for several key features of model development and application has been illustrated and is now leading to enhanced activities in several key areas, such as climate [*Cramer*, 1996; *Cramer et al.*, 1996], soils [*Scholes*, 1996], and land use [*Turner et al.*, 1995]. A particular area where better data products are achievable and urgently needed is the wealth of site-based observations of biogeochemical fluxes. As a direct spin-off from the Potsdam comparisons, an international team, the Global Primary Production Data Initiative (GPPDI) is now developing a new collection of harmonized observations of such variables, as well as improved methods to make this data useful at the broad scale required for global applications [*Olson and Prince*, 1996; *Prince et al.*, 1995].

ATMOSPHERIC TRACER TRANSPORT MODEL INTERCOMPARISON PROJECT

OVERVIEW

The Atmospheric Tracer Transport Model Intercomparison Project (TransCom) is a special project of the International Geosphere-Biosphere Programme (IGBP), under the Global Analysis, Interpretation, and Modeling (GAIM) Task Force.

The objective of TransCom is to reduce uncertainties in the global budget of atmospheric CO_2 that result from differences among tracer transport models that are used in 3-dimensional "inversions" of the observed spatial and temporal variance of CO_2 concentration. An initial set of two experiments was performed using 12 models, and involved an aseasonal northern hemisphere source (fossil fuel emissions forced by fluxes derived by Inez Fung from emission the inventories of Marland, 1989) and a seasonal biotic source (annually balanced net ecosystem exchange with the terrestrial biosphere according to [*Fung et al.*, 1987]. The intent of these experiments was to use the "fossil fuel" simulation to compare the annual mean spatial structure among the models, and to use the "biosphere" experiment to document the behavior of the simulated seasonal cycles. The results of these initial experiments have been analyzed, were presented in a poster by Law, Rayner, and Enting at the IGBP/GAIM Science Conference [*Rayner and Law*, 1995].

Thirteen modeling groups from six countries participated in the recently completed Phase 1 of the TransCom project, and have published a Technical Report on our findings [*Rayner and Law*, 1995]. We found a surprising level of disagreement among the simulations of the effects of fossil fuel emissions and seasonal terrestrial exchange on the spatial and seasonal behavior of atmospheric CO_2. These differences in simulated transport lead to uncertainties in estimates of the global annual sources and sinks in the natural carbon cycle that are comparable to those associated with estimates of air-sea exchange or global greening.

Our results have also shown that the uncertainties arising simply from passive tracer transport in atmospheric models are of the same order as those expected from differences in the reactive chemistry among CTMs. Atmospheric chemists and others interested in global trends and transport of trace species should be very interested in our results.

In order to quantify the mechanisms for the differences among the simulations, and to improve our confidence in the transport calculation, TransCom is now in its second phase which involves the simulation of the trace gas sulfur hexafluoride (SF6).

SF6 is emitted in trace amounts, mostly from electrical switching equipment [*Levin and Hesshaimer*, 1996; *Maiss and Levin*, 1994; *Maiss et al.*, 1996]. Unlike CO_2, the time series of SF6 is very simple and easy to interpret, and the sources are relatively well known. There are no known sinks. Unlike other anthropogenic tracers such as CFCs and krypton-85, the growth rate of global emissions is steady, so the concentration field is in equilibrium. This gas is therefore ideal for testing tracer transport models.

We have drafted an experimental protocol, including a set of required model outputs that will elucidate the mechanisms that produce differences among the simulated concentration fields in the models. Preliminary results from these simulations are now available. Further interpretation of these results are underway and will be included in an upcoming special issue of the journal Tellus devoted to papers presented at the September CO_2 meeting in Cairns Australia.

FINDINGS

There is qualitative agreement among the models with regard to the annual mean meridional distribution of the "fossil fuel" tracer at the surface, which is encouraging given the importance of this

variable for inversion calculations. Nevertheless, the simulated hemispheric mean response at the surface varies among the models by nearly a factor of 2. Even the qualitative agreement among the models in the fossil fuel experiment breaks down when the three-dimensional structure of the tracer is considered. Variations in seasonal behavior of CO_2 in the "biosphere" experiment are even more pronounced, especially over continental regions which lack observational constraints.

The annual mean meridional response of the models to seasonal biotic forcing defines two mutually exclusive scenarios. Models which represent turbulent mixing in the planetary boundary (PBL) simulate an Arctic-to-Antarctic gradient in surface CO_2 that is roughly half as strong as that obtained in the fossil fuel experiment. The other models simulate a very weak meridional structure in these runs. Both resolved transport and sub-grid scale "column physics" are important in determining the responses obtained by the models to the prospected forcing.

The Atmospheric Tracer Transport Model Intercomparison Project (TransCom) was begun in 1993, to investigate the differences among models of three-dimensional atmospheric transport of CO_2 that are used to deduce the global carbon budget from observations. There are currently 13 modeling groups from six countries participating in TransCom. We have recently completed Phase 1 of our program, and have published a Technical Report on our findings[*Rayner and Law*, 1995]. We found a surprising level of disagreement among the simulations of the effects of fossil fuel emissions and seasonal terrestrial exchange on the spatial and seasonal behavior of atmospheric CO_2. These differences in simulated transport lead to uncertainties in estimates of the global annual sources and sinks in the natural carbon cycle that are comparable to those associated with estimates of air-sea exchange or global greening.

In order to quantify the mechanisms for the differences among the simulations, and to improve our confidence in the transport calculation, TransCom is now entering its second phase. We have begun a series of simulations of the trace gas sulfur hexafluoride (SF6), which is emitted in trace amounts, mostly from electrical switching equipment [*Maiss and Levin*, 1994]; Levin and Hesshaimer, submitted). Unlike CO_2, the time series of SF6 is very simple and easy to interpret, and the sources are relatively well known. There are no known sinks. Unlike other anthropogenic tracers such as CFCs and krypton-85, the growth rate of global emissions is steady, so the concentration field is in equilibrium. This gas is likely to be ideal for testing tracer transport models.

OBJECTIVES

The primary objective of the TransCom Project is to reduce uncertainties in the global carbon budget of the atmosphere that result from differences among models of chemical tracer transport. In support of this objective, the following tasks were defined:

- Evaluation of the realism of the various simulations of annual mean tracer distributions resulting from the aseasonal anthropogenic source used in the initial "fossil fuel" experiment. This involves a model calibration using a different trace gas.

- Investigation of the mechanisms responsible for producing the large discrepancies among the model responses obtained in the initial experiments. This involves both a careful analysis of the initial results and new sensitivity experiments designed to quantify the influence of various aspects of the model transport.

- Identification of key measurements which would result in the greatest reduction in the uncertainty associated with atmospheric inversion calculations.

- Recommendations for process-oriented research to improve the representation of global scale chemical tracer transport, and to further reduce uncertainties in global carbon budget calculations.

MODEL DESCRIPTIONS

Ten modeling groups have submitted results for the SF6 experiment to date, including most of the participants in the TransCom 1 intercomparison as well as several new models (Table 1). On-line models (CCC, CSU, and GFDL-SKYHI) simulate tracer transport in a fully prognostic GCM, calculating winds and subgrid-scale transport on time steps of minutes. Off-line models calculate tracer transport from either analyzed winds (NIRE, TM2, TM3) or GCM output (GFDL-GCTM, GISS, GISS-UVIC, MUTM). The off-line models are able to use much longer time steps, and specify input wind fields with frequencies varying from 1 hour to 1 day. Subgrid-scale vertical transport was parameterized in all models, using a variety of techniques. Off-line models generally include schemes to calculate these terms from the prescribed wind input, whereas online models calculate subgrid-scale transports at the same time as the dynamical calculation of the GCM winds.

ANU: The Australian National University chemical transport model	The ANU-CTM includes a stochastic Lagrangian advection scheme to move air parcels representing a known mass of tracer inair according to a wind field, derived from ECMWF data, on a 2.5 by 2.5 degree latitude/longitude grid with seven vertical levels at 1000, 850, 700, 500, 300, 200 and 100 hPa. The wind field includes a mean and time varying component. Conservation of tracer mass is accounted for by definition in the Lagrangian transport scheme so no mass fixer is required. The model surface layer is defined as spanning 1000-925 hPa. The model results were run from an initial condition of 350 ppmCO_2 for 5 years. TRANSCOM model results are taken from the fifth year of the model run.
CSIRO9: The CSIRO Division of Atmospheric Research GCM	Online tracer transport, semi-lagrangian. 56 gaussian latitudes, 5.625 deg longitude, 9 vertical levels.
CSU: The Colorado State University GCM	The input data sets were prescribed as surface fluxes to a low resolution (7.2x9 degrees, 9 levels) version of the CSU GCMand run for 10 years starting from a globally uniform initial condition. The end of the 10-year low resolution run was used as an initial condition for a 4 year run on a 4x5 degree, 17 level grid. The data submitted are monthly means for the final year at 4x5. Time step in the 4x5 model was 6 minutes, with cumulus mass flux specified at 1 hour intervals. PBL depth and turbulence kinetic energy were prognostic variables, so the surface values are for a variable depth PBL, not a fixed pressure level.
GISS: The GISS tracer model version used at CSIRO Division of Atmospheric Research	Offline tracer transport. 8x10 deg grid run with winds from GISS 4x5 deg GCM simulation. 9 levels.
MUTM and MUGCM: The Melbourne University Offline and Online Models	The Melbourne University tracer model (MUTM) is derived from the Melbourne University GCM (MUGCM) which isrhomboidal, 21 wave resolution with 9 vertical levels. The tracer model runs with wind and convection statistics taken from MUGCM and input daily to tracer model. The tracer model is described in Law,R., I. Simmonds, W.F. Budd, 1992: Application of an atmospheric tracer model to the high southern latitudes. Tellus, 44B, 358-370.
NCAR: The NCAR CCM2 GCM with tracer	Online semi-lagrangian tracer transport. T42, 2.8x2.8 deg grid. 18 vertical layers. Convection, vertical diffusion, PBL subgrid processes.
NIRE: The National Institute for Environment and Resources tracer model (Japan)	The global three-dimensional model used in this study was developed by the National Institute for Resources and Environment during the 1993 Fiscal year (NIRE-CTM-93). The meteorological data analyzed at the European Centre for Medium Range Weather Forecasts (ECMWF/TOGA/Advanced) are used to transport and convect the minor constituent. Vertical resolution is 15 sigma levels extending from 0.975 to 0.02. Horizontal resolution is 2.5x2.5 degrees. Time resolution is 6 hours. A semi-Lagrangian scheme is adopted to calculate a transport process. A non-local planetary boundary layer is used to convect minor constituents near the surface.
TM2: The Hamburg tracer model	The calculations were performed with the Hamburg TM2 tracer model version 8.5, using the "fine grid" resolution: 4 deg latitude by 5 deg longitude and 9 sigma layers in the vertical dimension. The employed meteorology is from the analyses of the ECMWF for the year 1986. Each source was run for four years, with initial concentration set to zero. The deposited fields are from the fourth year. The fields on the pressure levels have been linearly interpolated from the models sigma levels (using a mean annual surface pressure field). The surface layer is defined as the lowest sigma level extending typically between 1000 and 950 hPa in this 9 layer model version.
TM2Z: The CFR/LMCE - FRANCE version of the TM2 tracer model	Resolution of the model is 2.5x2.5 degrees x 9 is 0 sigma levels. Two years, 1990 and 1991.

The TM1 tracer model

Simulations were performed using the TM1 tracer model version 7.1 which was described in detail by Heimann and Keeling(1989). TM1 has a horizontal resolution of 7.9 degrees (180./23.) latitude by 10 degrees longitude, 9 sigma layers in the vertical, and a numerical time step of 4 hours. Wind fields are updated every 12 hours, sources every 24 hours.

The wind fields are based on meteorological observations on a 1.825 x 1.825 degree grid processed by the four-dimensional data assimilation system of the European Center for Medium-Range Weather Forecasts (ECMWF) for the Global Weather Experiment (GWE) from December 1978 through November 1979.

Vertical convection is described by a set of monthly transition matrices retained from a previous version of the tracer model, which used wind fields generated from a three-dimensional general circulation model (GCM) of the atmosphere developed for climate studies by Hansen et al. (1983). Following Heimann and Keeling (1989), I have reduced the convective matrices globally to 0.50 of their original values. There is no explicit boundary layer in the model.

The model variant used here included explicit horizontal diffusion coupled to vertical convection in the same way as described by Prather et al. (1987). This variant was used in Keeling et al. (1989) (e.g., labeled 'standard scenario' in figures 65 and 66,p. 349, and referred to in Table 7, p. 338 as 'with horizontal diffusion') and in i Iacobellis et al., 1994 (JGR). This produced an interhemispheric exchange time for fossil fuel of about 1.1 years (without explicit diffusion, the interhemispheric exchange time was about 1.4 years).

Each source was run for 4 years with initial concentration set to 0. The fields supplied to Transcom are for the fourth year;results are expressed in ppm. Surface fields were taken from the lowest model sigma level, typically extending between 1000 and 950 hPa. The fields at 200 and 500 hPa were linearly interpolated from the model sigma levels using a mean annual surface pressure field.

Fossil source

The global annual total was 5.276 GtC/year (for earth radius of 6375 km) The README file for the original Giss source indicate that the source is about 5.5 gtc/year; I assume that they used a different value for the earth radius than I did.

ff_surff.XX surface
ff_500mb.XX 500 hPa
ff_200mb.XX 200 hPa

where XX = 01 to 12 for Jan to Dec, and 13 for annual average

Seasonal biospheric source

The original monthly Giss values were taken as mid-month values. Since my runs are for 1979 with 365 days, I have assigned the Jan to Dec mid-months to days 16.,35.5,75.,105.5,136.,166.5,196.,228.,258.5,289.,319.5, 350., respectively. I wrapped the data by assigning the Dec value to day -15. and the value for Jan to day 381 and then linearly interpolated daily values between the mid-months to give 365 daily values. The annual total of the source was adjusted to zero in each model box.

biosurff.XX
bio500mb.XX
bio200mb.XX
where XX = 01 to 12 for Jan to Dec, and 13 for annual average

MODELLING THE METHANE CYCLE

Insights provided by the results of the Transport Code Intercomparisons set the stage for developing models of the methane cycle. Methane is simpler in one respect than the CO_2 cycle in that it does not have large and poorly constrained sinks in the ocean and terrestrial systems. However, methane is not conservative in the atmosphere, being subject to oxidation.

The atmospheric chemical interaction of methane is being studied in a joint GAIM/IGAC 3-D model intercomparison activity. This study focuses on the atmospheric response to changes in emissions, and therefore links naturally to the proposed methane cycle study. For instance, 3-D model estimates of temporal and spatial variations of methane oxidation can be used together with observed variations of methane to estimate emissions from wetlands.

As a first step in exploring the methane cycle, we focus on terrestrial sources. The largest sources are natural and artificial wetlands. Thus, we began by concentrating our attention on wetlands.

Wetlands

The methane budget is strongly affected by wetland sources, both natural and anthropogenic. Consequently, in order to correctly account for methane terms in global biogeochemical models, it is essential to understand the role of wetlands in methane production as well as the effect of changing wetland distribution. The extent of wetlands is uncertain because there is no clear basis for identification and classification of wetlands on a global scale. In addition, the areal extent of wetlands is being modified as a result of land-use changes, so that once a globally consistent classification scheme is established, the areal distribution must be monitored and recompiled. New data are becoming available from remote sensing which provide a global perspective on wetland distribution and classification, but which are not yet reconciled with ground-based ecological and hydrological data. There remains a gulf between the scale of trace gas emissions as measured from the ground, and the measurable atmospheric effects of this based on remote sensing. These conceptual and technical discontinuities need to be reconciled.

Detailed maps of wetlands are available for the U.S. and Europe and regional maps are available for most of the world. However, these maps are almost always static and based on floristics rather than function. We need current and ongoing monitoring of wetland extent and flooding, with classification based on biogeochemical function. Such information is now obtainable with remote sensing in conjunction with regional data on soils, climate, and vegetation. While some studies are addressing the global effect of atmospheric exchange of trace gases from wetlands, most have been concerned with wetlands at a local level.

Newly available remotely sensed data provides the opportunity for major advances in the classification distribution of wetlands. Passive and active microwave remote sensing provides the capability of mapping inundation extent seasonally to monitor natural and anthropogenic (agricultural) variations. These are critical data because in many regions, the amplitude of natural seasonal variations are equal to or greater than the long-term anthropogenic modifications. Also, SAR data allow classification of vegetation phenology.

As a first step, we have constructed a wetland functional classification scheme (Fig. 1).

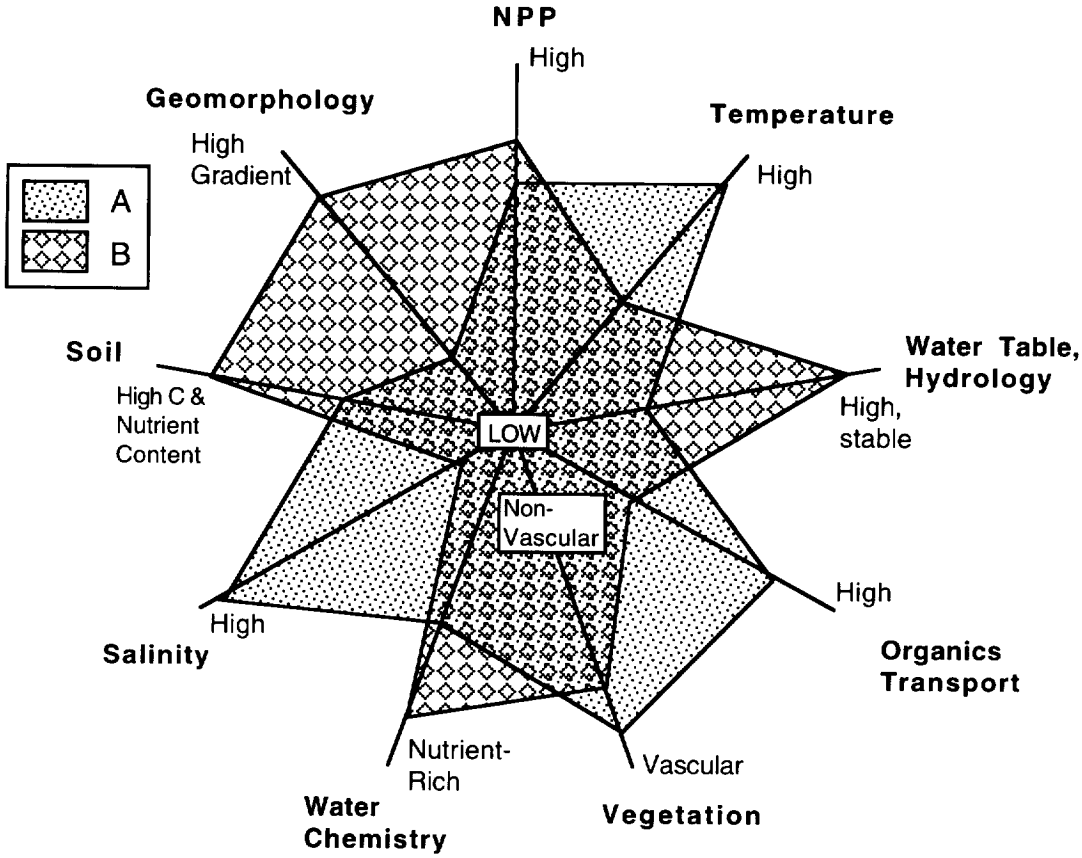

Figure 1. Graphical representation (2-D) of 9-dimensional parameter space for wetland parameterization scheme. Two wetland functional types are shown. Type A has high salinity, high proportion of vascular plants, high temperature, etc. Type B has low salinity, high gradient in surrounding regions, high soil carbon & nutrient content, etc. Any wetlands with similar shapes on this 9-dimensional representation are postulated to have the same set of functional processes (controlling CH_4, CO_2, N, S) regardless of where they are found. However, wetlands with different shapes on this representation can also share the same functions with appropriate trade-offs between the various parameters. The quantitative relationships (P_j) between the effects of the nine parameters have not yet been established, and represent a primary research goal in future investigations of wetland processes. (From Sahagian, unpublished)

This, in conjunction with developments in understanding of emissions from rice paddies and ruminants will provide the input boundary flux for atmospheric methane necessary for climate and biogeochemical models. This flux can be balanced against oxidation and atmospheric accumulation, as modulated by atmospheric transport, to be provided by the transport codes.

With sources, sinks, and atmospheric transport terms in hand, methane cycle models can be developed which will accurately predict atmospheric methane concentration evolution in response to human activity as well as natural causes.

The following models have been compared with respect to transport of fossil fuel and seasonal terrestrial forcing of CO_2:

ANU: Australian National University chemical transport model

CSIRO9: CSIRO Division of Atmospheric Research GCM
CSU GCM: Colorado State University General Circulation Model
GFDL: GFDL tracer model (run at CSIRO)
GISS: NASA GISS tracer model (run at CSIRO)
MUGCM: Melbourne University General Circulation Model
MUTM: Melbourne University Offline chemical transport model
NCAR: NCAR CCM2 GCM with tracer
NIRE: National Institute for Environment and Resources (Japan) model
TM1: TM1 tracer model (Scripps Inst. Oceanography)
TM2: Hamburg tracer model
TM2Z: CFR/LMCE - FRANCE version of the TM2 tracer model

All 12 modeling groups are expected to participate in the upcoming SF6 calibration experiments. In addition, another group has been added: LMD: Laboratorie de Meteorologie Dynamique (France) GCM

Appendix 1

Participants in the African Modelling Workshop

Appendix 1
Participants in the African Modelling Workshop

NAME	DATE: March:	TALK TITLE
Abdellaoui Abdelkader	7	Land-use changes in urban environment
Akin Adewale	6	Monitoring climate and anthropogenic impacts on the hydrological environment
Ayije-Lo Ajavon	10	Trace gas profiles in tropical Africa
Abigail A. Amissah-Arthur	7	Land use changes in West Africa: Evolution of crop-livestock production systems in the moist savanna
Rachid Boukchina	7	Modeling of Nonpoint-Source Pollution From AGRO-Ecosystem: Case of Nitrate
Geoffrey M. S. Chavula	6	The impact of climate change on water resources of Malawi: Vulnerability assessment and adaptation strategies
James Gambiza	5	The Regeneration of Zambezi Teak Forests After Logging: The Influence of Fire and Herbivory
Willy S. Goma	6	Quantification of the Role of Land-Use Dependent Moisture Feedback on the Atmospheric and Hydrological Water Balance Over the Zambezi River Catchment
Chemist Gumbie	5	Forestry
Kinfe Hailemariam	7	Impact of climate change over Awash river basin
Suman Jain	10	GHG emissions from energy sectors in Zambia
Alec Joubert	10	Equilibrium and transient climate change scenarios for Africa south of the equator
Jenesio I. Kinyamario	4	Soil carbon and impact of climate change on grassland production
Kwame Mensah Foster	6	Monitoring land use and forest cover using satellite imagery
N. Emmanuel Ngwa	7	The use of remotely sensed information in monitoring local community efforts in managing baseline natural resources in western Cameroon
Michael Ocaido	5	Developing predictive models for ticks and tick-born diseases in mixed game and livestock areas around lake Mburo national park, Uganda
Placide Corneille Oke	5	Climatic change and human health
Daniel O. Olago	11	Late quaternary glacial-interglacial cycle of climatic and environmental change on Mt. Kenya
Kefa V. O. Rabah	4	Regional carbon cycle model for Africa
Eston Sambo	6	Developing Strategies for Management of the Lake Chilwa Basin (An Inland Drainage Lake) in Malawi
Mogodisheng B. M. Sekhwela	6	Woody biomass and utilization aspects in Botswana: Can these be modeled?
Lerato Thahane	8	The Development of an Integrated Range Condition and Preferred Management Density Model for Thekudumae District, Northwest Province, South Africa
Mame Demba Thiam	8	Set-up of a GIS for Drought Monitoring in the Northern Part of Senegal
Otlogetswe Totolo	4	Assessment of Soil Within Eroded Areas in the Gumare Area(West of the Okavango Delta in Northwest Botswana)
Pius Yanda	4	The effect of soil erosion on soil quality in semi-arid environments-The Case of Mwisanga Catchment, Central Tanzania

Appendix 2

Abstracts from African Workshop Participant Presentations

Appendix 2
Abstracts from African Workshop Participant Presentations

Land Use Changes in Urban Environment

Abdelkader Abdellaoui
Dept. of Geography; Sc. And Tech Uni. Of Algiers; B.P. 32 El Alia 16111 Algiers Algeria
phone: (213) 2 95 91 28; fax: (213) 2 51 58 65

ABSTRACT
Cities are the sites of the most intense alteration of the natural environment due to land use and other anthropogenic activities. In developing countries, the population increases very quickly; inducing several needs (shelter, clothing, food). This, in turn, causes a permanent variation of the environment. In Algeria, for example, the population was 10.2 million in 1962; it was 16.9 million in 1967, 23 million in 1977 and 28 million in 1987. The growth rates, measured in ten year intervals, rose to 3.8% from 1967-1977, 3.1% from 1977-1987, and finally 2.3% from 1987 to the present year. Although this percentage has decreased over time, the statistic still reflects an elevated rate of growth. Thus, resulting in a permanent apparition of new urban centers along with a rapid extension of existing cities.

To examine the effect of urban expansion on the environment, two examples were studied. The models included the urban complex of Blida which is situated on an agricultural zone in Mitidja, 50 km from the Mediterranean sea, and the oasis of Laghouatt; situated 400 km south of the Mediterranean coast in the semi-arid region. Before 1962, Blida encompassed what is now known as Blida, along with many other small cities. Since that time, the city has expanded 1055 hectares. These hectares were previously tagged for agricultural use. The oasis of Laghouat was originally built around gardens and city; yet due to it's expansion, there is almost no agricultural land remaining. To study the spatial extension of urban space we combined the traditional data (maps) with satellite images; yet several problems arose: 1) in residential districts, the spectral response appeared to be equal to that of vegetation. This can be attributed to pixel heterogeneity. To resolve this problem we characterized the relationship between individual pixel constitution and spectral response. 2) In non-concentrated urban space, confusion in distinguishing between buildings, bare soil, and agricultural space was found. To resolve this problem we used an algorithm based on pattern recognition. 3) In presaharan and mountainous areas there was confusion in distinguishing between buildings and rocks. To resolve this problem we developed an urban index based on the stretching and spectral responses of buildings.

Monitoring climate and anthrophogenic impacts on the hydrological environment

Akin Adewale
AFRICAN GAIM MODELLING WORKSHOP
March 3-12 1997 Mombasa, Kenya

One of the most important advantages of remote sensing techniques over contemporary traditional techniques in data acquisition is monitoring capability. A number of remote sensing applications have been carried out in hydrological sciences including surface water resource inventory.

In this study, an investigation was made into the application of this remote sensing monitoring capability in assessing changes and trend of change in the measures of the surface water resource of the Sokoto River drainage basin. This occurred during the years of 1956, 1975 and 1986. This basin, representative of drainage basins in the semi-arid lands, is characterized by climatic variation and inadequate data bases. This has not permitted an efficient planning of its water resources.

Using two year anniversary data Landsat MSS imageries (1975, 1986) coupled with the 1956 topographic map as the base, an inventory and monitoring of the upper Catchment of the Sokoto River basin has been attempted at a reconnaissance scale. A decline of about 50% in the drainage parameters of the basin between 1956 and 1975 was obtained, while for 1975 to 1986, the decline was less than 20%. Also a rate of decline of 0.6% per annum in the drainage basin's linear characteristic has been obtained. The various indices of the drainage basin's linear characteristics that have been determined over the three periods (1956, 1975 and 1986) were consequently analyzed using the Analysis of Variance (Anova) statistic. This was done with the aid of a statistical software - `Microstat' on a personal computer.

The impact of the 1967-1985 Sahelian drought vis-à-vis that of the Bakolori reservoir and irrigation projects established in 1978, over the basin were considered in the analysis. It was observed that the Sahelian drought has a significant negative impact on the basin. The impact of the Bakolori reservoir and irrigation projects is difficult to ascertain as to positive or negative with any statistical significance. The results of the Anova analysis for the data showed significant changes between 1956 and 1986 vis-à-vis the stream length over the basin. A computed ratio of 8.336 was obtained as compared with a theoretical `F' ratio of 6.94.

Based on the above analysis (Anova results), the null hypotheses of Nos. 1 and 3 were rejected while the null hypotheses Nos. 2 and 4 were accepted as valid as put forward in the course of investigation.

It is expected that the efficiency of this technique, as well as data from this study will provide useful input into semi-arid water resources modeling schemes.

TRACE GAS PROFILES IN TROPICAL AFRICA

Ayite-Lo Nohende AJAVON
Atmospheric Chemistry Laboratory
Faculte des Sciences, Universite du Benin, B. P. 1515 Lome, TOGO

The tropospheric concentrations of most reactive chemical species have been found to vary in space and in time all over Tropical Africa. Two categories of chemical species play a major role and are most involved in Africa Tropospheric Chemistry: Trace gases and Aerosols:

• Trace gases result primarily from biomass burning, engine exhausts, factory smokes. CO, CO_2, CH_4, NO_x, NO_y, SO_x, O_3, NMHC, VOC, $R(CH)_x$ and Aromatics are the major trace species encountered.

• Aerosols originate from biomass burning, harmattan dust , open-air house solid waste incineration and vehicular traffic of unpaved as well as unswept paved roads and are composed of TPM, POC, SO_x, C_{soot} and elemental C. Severe visibility reduction, increased respiratory diseases and chest congestion complaints are usually recorded.

The high concentration and the large scale increase of tropospheric ozone observed from data of field measurements campaigns performed in Tropical Africa indicate fundamental change in the chemical behaviour with perturbation of oxidant cycles in Africa troposphere, leading to important photo chemistry and climate change.

Tropical Africa atmospheric phenomena impacts are going to play an important role in global climate for several reasons:

• Emissions of industrial and agricultural atmospheric pollutants are expected to increase very strongly in the next few years,
• Chemical use and factory emissions are increasing out of control,
• Solar UV fluxes, higher temperatures and water vapor content are important,
• Convection processes are at a maximum in the tropics, providing fast and efficient vertical transport for pollutants from the surface to high altitudes, and
• Biomass burning activities are widespread in tropical Africa.

Data from collected rainwater analysis reveal high acid values comparable to those of industrialized countries. Formic and Acetic acids from biomass burning account for more than 50% of tropical African rain acidity.

If data from field measurements campaigns can provide very useful information about trace gases and atmospheric chemistry in Tropical Africa, we must recognize that they remain scarce and very far from representing the amounts of chemical species involved by anthropogenic activities.

Land Use Changes in West Africa: Evolution of Crop-Livestock Production Systems in the Moist Savanna.

Abigail Amissah-Arthur
International Institute of Tropical Agriculture, Ibadan, Nigeria

Introduction

West Africa contains the largest area of arable farm and grazing systems, suitable for cropping, in the region. On this land, traditionally crops and livestock have been functionally linked, but operationally separated enterprises. However, many of the traditional exchange relationships between pastoralists and crop farmers are disappearing (Powell and William, 1994). Increasing human populations on a finite land base combined with long term climate changes are transforming the specialized systems, based on extensive shifting cultivation and grazing, to more integrated and intensely managed enterprises. Improved crop-livestock production systems are currently developing to satisfy the growing demand for food and prevent the degradation of the natural resource base. According to Winrock International, the greatest opportunity for sustainable increases in agricultural productivity in sub-Saharan Africa lie in agricultural intensification through the evolution and maturation of a mixed crop - livestock farming system.

Development strategies that aim to raise the productivity of specific mixed crop-livestock systems must carefully consider the stage of development of the target area in relation to intensification, and the nature of crop-livestock interactions. Although crop - livestock production systems are evolving as dominant systems, the future imperative of intensification of agriculture indicate a need to develop technologies to meet the demands of these new systems of food production. One perspective on appropriate technology development for crop-livestock production systems is to adopt a resource management approach where land is considered the most critical resource. The land must be managed to optimize crop and livestock returns in a sustainable manner. Improving natural resource management in the moist savanna demands a better understanding of not only the complementary and biological factors (i.e. crop residue for animal feed, and deposition of manure on cropland for soil fertility maintenance), but also the non-complementary interactions involving competition for land, labor, capital and communal resources. Beside these interactions which on their own have important implications for resource management, there is a need for understanding the process by which farmers gain access to, and use natural resources for producing crops and livestock. By examining the manner in which land-use, feed, and soil fertility are managed in the production of crop and livestock the proposed study aims at providing insight into the factors that guide farmers' resource use and management decisions and the manner in which resource use and management are evolving in response to biophysical and socioeconomic change.

MODELLING OF NONPOINT-SOURCE POLLUTION FROM AGRO-ECOSYSTEM: CASE OF NITRATE

Rachid Boukchina
Institute of Arid Lands - Nahal 6051 Gabes Tunisia

Agriculture contributes to non-point source pollution of water resources through leaching and runoff of crop nutrients, pesticides, animal wastes, and through soil erosion from cropland. Development of effective solutions to water quality problems resulting from agricultural land-use requires an appropriate multi-disciplinary approach involving interaction between the components and process of the natural environment and specific human activities associated with land use.

We have developed a numerical multi-disciplinary approach in view of simulation nitrate output from agriculture watersheds through a conceptual model. The simulation of nitrate nonpoint-source pollution requires the coupling of a nitrogen cycle in agriculture ecosystem with a hydrological distributed parameter model. For this, we have used the CEQUEAU (Morin et al, 1981) hydrological model. The CEQUEAU model takes into account the spatial physical variability of the watershed through subdivision in cells of square areas. For each cell, the model simulate the soil water budget. A further cell subdivision into partial cells or fields according to sub-basin is required to allow the determination of the down stream routing from one field to the next. The nitrogen cycle subroutine integrated to CEQUEAU model includes the major process governing nitrogen inputs (organic and mineral fertilizers and atmospheric deposition) internal transformations (mineralization, nitrification and immobilization) and outputs (plant uptake, denitrification, leaching and runoff exportation) for each field over the watershed. Using two year-data from monitoring agriculture watershed (78 hectare), the obtained results showed that the model was able to simulate the seasonal variation of nitrate concentration in runoff accurately.

The regeneration of Zambezi teak forests after logging: The influence of fire and herbivory.

James Gambiza, University of Zimbabwe, PO Box M P 167, Mt Pleasant, Zimbabwe.

Zambezi teak forests are confined to Kalahari sands and occupy 5.1 percent of the Zimbabwe. These forests contain important timber species such as Guibourtia coleosperma, Pterocarpus angolensis and Baikiaea plurijuga. Concern has been expressed about the poor regeneration of these forests. The impacts of fire and herbivory after logging on the regeneration of the commercial species were being studied. The hypothesis that fire and competition between timber species and other plant species reduces regeneration after logging was being tested.

Four early burning treatments with different fuel load levels were applied to 50 m x 50 m plots just after the end of the 1992/93 growing season. The treatments were: (1) no burning; (2) burning using the natural fuel load; (3) burning after clipping all herbaceous plants to 5 cm (to simulate intense grazing), and (4) burning using twice the natural fuel load. Treatments were replicated three times and applied in a completely randomized block design.

A control (no grazing) and nine treatments involving three times of grazing and three stocking rate levels were applied to one hectare plots in a completely randomized factorial design with three replications. Cattle (preferential grazers) and goats (intermediate feeders preferring browse) were used.

Competition between seedlings of timber species and other plants was studied in an area of 1 hectare. Four treatments were applied to 20 m x 20 m plots in a completely randomized design with four replications. The treatments were: (1) all above-ground shoot material except for the timber species was regularly removed; (2) all above-ground woody material except for the three timber species was regularly removed; (3) all above-ground herbaceous material was regularly removed, and (4) control (no plants removed).

Preliminary indications are that fire and drought are the major factors reducing regeneration of the teak woodlands. Establishment of seedlings of timber species was poor because of drought. The few seedlings (less than 5%) that had germinated were killed by mice. Seedling establishment is apparently an episodic event that is dependent on rainfall.

Time of grazing and stocking rate had significant effects on grass fuel loads. Cattle and goats did not browse timber species. Browse selection patterns were unrelated to chemical composition of the leaves.

A model of the dynamics of logged Zambezi teak forests will be developed. The impacts of large herbivores, fire and frost on key processes such as seed production, dispersal, germination, establishment, mortality, growth rate of different size classes and competition among individuals will be synthesized into a model of the population dynamics of timber species.

QUANTIFICATION OF THE ROLE OF LAND-USE DEPENDENT MOISTURE FEEDBACK ON THE ATMOSPHERIC AND HYDROLOGICAL WATER BALANCE OVER THE ZAMBEZI RIVER CATCHMENT

Willy S. Goma
Department of Meteorology
P.o Box 310095, Lusaka 15301, Zambia

Over the last 50 years, a number of climate anomalies have occurred over the globe in general. Over Zambia extreme events have been experienced resulting in both active and weak as well as good and bad seasons. The much talked about global warming may be responsible for changes in pressure, wind and moisture patterns which can be linked to the observed precipitation anomalies.

To detect changes in rainfall pattern, diagnosis of the rainfall trend over Zambia has been made over selected regions. Mean seasonal rainfall data was obtained from conventional ground based rain-gauges which are spread throughout the country. In addition to rainfall, mean air temperature was also constructed to observe variation in air temperature. The rainfall season (December, January, February and March) were considered. Correlation coefficients between stations were calculated. Mutually and highly correlated stations identified were grouped together to form coherent regions for analysis.

The observed global temperature records, including ocean and land readings, revealed a warming trend during this century of a magnitude within the range predicted by models (ACTS, 1990). Furthermore, the latter half of 1980 registered the warmest temperatures on record (acts, 1990). In Zambia, as well, mean annual air temperature has risen from around 28 degrees centigrade (1950-1974) to around 29.5 degrees centigrade between (1982-1994) over the region (14.0 s- 18.0s). There was a reduction in mean annual air temperature between (1972-1982) with the lowest being around 26.5 degrees centigrade. The same selected regions show a reduction in mean seasonal rainfall between 1950 and 1978. The mean seasonal rainfall was around 800 mm and after 1978 dropped to 600 mm. The highest rainfalls reported (1950-78) were over 1,000 mm in 1952/53, 1971/2, 1975/76 and 1978/79. While between (1980-1994) the highest was around 800-900 mm during the 1987/88, 1988/89 and 1989/90 seasons. The lowest mean seasonal rainfalls, that fell to around 600 mm between 1950-1978, were in 1949/50, 1961/62, 1963/64, 1971/72 and 1977/78. However, between 1980-1992 the lowest was around 500 mm in 1981/82, 1983/4, 1986/87 and 1991/92.

Moreover, with these few observations, we intend to perform an interdisciplinary meteorological-hydrological research in order to quantify the role of land use-dependent moisture feedback on the atmospheric and hydrological water balance over semi-arid region of southeastern central Africa (Zambia/Zimbabwe). In particular, drought will be investigated to see if land use has contributed to the severity of drought, as they affect the continental moisture recycling. The challenge is to distinguish between two processes affecting rainfall in the Zambezi catchment. First, how far trends in the moisture content of rain producing air masses are explained by decadal and vast land-use changes. Second, the impact of local (subcatchment scale) evapotranspiration on the rainfall distribution on the small scale will be quantified. It is hoped that with attendance of this African-GAIM modelling workshop the project will be a success especially that new software (hydro, Acru, Century) in hydrological modeling have been exposed to the author. (This proposed research will be jointly venture between Institute of Geophysics & Meteorology (German), Delft (Netherlands) and Zambia/Zimbabwe meteorological services.

Impact of Climate Change over Awash River Basin

Kinfe Hailemariam
National Meteorological Services Agency, P.O. Box 1090, Addis Ababa, Ethiopia

Scientific evidence indicates that due to increased concentration of greenhouse gases (GHGs) in the atmosphere, the climate of the earth is changing. A change in climate can alter the spatial and temporal availability of water resources. Therefore, qualitative estimates of hydrologic effects of climate change are essential for understanding and solving the potential water resource problems.

In this experiment an attempt has been made to study sensitivity of water resources to climate change over the Awash River Basin.

Awash River starts over the highland of Central Ethiopia , about 150 km west of Addis Ababa, at an altitude of about 3000 m above sea level and ends in Lake Abe at the border with Djibouti Republic, at an altitude of about 250 m above sea level. The total length of the river is about 1200 km and its catchment area is 113700 km2. The climate of Awash varies from humid sub-tropical to arid.

The basin has been divided in to three sub catchments; for a better resolution in calibration & simulation routine. Station based meteorological data were organized into area averages, Grid method GRASS's inverse distance weighing technique is used to obtain area rainfall. Simple arithmetic mean is used to derive area values for the other meteorological parameters. Different sets of temperature & rainfall scenarios were developed using GCM (both transient and CO_2 doubling) and incremental scenarios. IASSA integrated Water Balance model (WATBAL) is used to produce runoff scenarios under changed climate.

The model represents water balance streams from the use of continuous functions of relative storage to represent surface outflow, sub-surface outflow, and evapo-transpiration. In the model, the mass balance is written as a differential equation, and storage is lumped in a single mass balance. All components of discharge and infiltration are dependent upon the state variable, relative storage, with exception of base flow which is given as a constant in the mass balance equation. The model contains only three parameters e, a, and S_{max} which are related to surface runoff, subsurface runoff, and maximum catchment water holding capacity, respectively. The model has been calibrated using 10 year periods (1970-1980), validated for another 6 year period (1981-1986), and then simulated under different climate scenarios.

Results of impact assessment study over the basin showed a decrease of runoff projection by most of the GCM, which ranges from -10% to -34%, with doubling of CO_2 and transient period (GFD3, CCCM, GF01), where as UK89 projected a 40% increase. Sensitivity analysis based on incremental scenarios showed a drier & warmer climate change scenario which result in a reduced runoff, with high dependence on the rainfall.

GREENHOUSE GAS EMISSIONS FROM THE ENERGY SECTOR IN ZAMBIA

SUMAN JAIN, MATHEMATICS DEPT, UNIVERSITY OF ZAMBIA

The Zambia Country study on Climate Change under the U.N. convention on Climate Change was carried out by the funding of G.T.Z in two stages: (1) preparation of inventory of GHG emissions in Zambia (2) Abatement costing through possible mitigation options. Using the IPCC methodology, it was estimated that the total CO_2 emissions from the consumption of coal and coke in 1990 were 853.37 Gg and 86.5 Gg respectively. The estimated emissions of CO_2 from liquid fuels in 1990 were 1859.48 Gt. The estimated CH_4 emissions from coal mining in 1990 were 0.316 Gg. Biomass being a potential source of energy in Zambia, GHG emissions from biomass in the form of burning wood as fuel, consumption and production of charcoal were also estimated. The estimates of CH_4 and N_2O from biomass used as energy in 1990 were as follows:

Fuel	CH_4 (Gg)	N_2O(Gg)
Wood for direct use	44.68	0.31
Charcoal consumption	0.888	0.05
Charcoal production	29.76	0.04

Although CH_4 emissions from biomass are much smaller in weight than CO_2 emissions from either solid or liquid fuels, its importance in mitigating the GHG effect should not be underestimated. The global warming potential(GWP) of CH_4 is about one or two orders of magnitude larger than that of CO_2 and depending on the time frame one chooses. Therefore the above amount of CH_4 produces more global warming than the CO_2 from fossils. Use of biomass as energy is one potential area which needs to be addressed for any mitigation strategy. This holds true in general for Africa region since biomass is a significant source of energy in Africa.

EQUILIBRIUM AND TRANSIENT CLIMATE CHANGE SCENARIOS FOR AFRICA SOUTH OF THE EQUATOR

Alec Joubert

Climatology Research Group,
University of the Witwatersrand, P.O. Wits, 2050, SOUTH AFRICA

Climate change scenarios based on several different general circulation models (GCMs) are provided for Africa, south of the equator (southern Africa). Estimates of climate change are based on both atmospheric GCMs linked to simple mixed-layer oceans and fully-coupled ocean-atmosphere GCMs. The mixed-layer models simulate the equilibrium response of regional climate to an instantaneous doubling of atmospheric carbon dioxide (CO_2). The fully-coupled models simulate transient response of the system to gradually-increasing concentrations of anthrophogenic greenhouse gases, and in some cases, sulfate aerosol forcing.

Possible Changes in Mean Temperature
Mixed-layer models simulate an equilibrium response to instantaneously-doubled CO_2 of 3-3.5C during the summer of the southern hemisphere (December-February). The transient response to gradually increasing greenhouse gas concentrations simulated by the fully-coupled is 1-2C. Most differences between mixed-layer and fully-coupled models are marked over the central subcontinent south of 15S, and over the southern oceans.

The Influence of Sulfate Aerosols
The direct forcing effects of sulfate aerosols have been incorporated in the Hadley Center for Climate Prediction and Research model by altering surface albedo over several regions of the globe including south central Africa. Over southern Africa, the effect of sulfate aerosol forcing as represented in the model is to reduce both the magnitude and rate of warming predicted for the subcontinent. Based on combined forcing due to increasing greenhouse gases and sulfate aerosol forcing, temperatures may be expected to increase by approximately 0.37C per decade between the present and at least 2060 (a rate which is higher than the global average).

Possible Changes in Mean Rainfall
Both equilibrium and transient climate change simulations indicate that summer rainfall may be expected to increase within the tropics by approximately 10%. Fully-coupled models simulate widespread decreases in summer rainfall over much of the subcontinent south of 15S of 10-15%, whereas mixed-layer models simulate broader regions of rainfall increases (10-15%). However, models of both types display very-little inter-model agreement over southern Africa in terms of the sign of predicted changes. The result is indicative of the problems associated with the representation of rainfall produced by connective processes within GCMs, and it's representation at the coarse spatial scales typical of all GCMs. Currently therefore, little confidence can be placed in estimates of rainfall changes based on GCMs alone.

Possible Changes in Diurnal Temperature Range
There is a marked seasonality in the simulated changes in diurnal temperature range over southern Africa. During the summer and Autumn (September-May), diurnal temperature range is expected to increase, indicating possible decreases in cloud cover, relative humidity, soil moisture, runoff and precipitation (see above). However, during winter (June-August) the diurnal temperature range simulated by the Hadley Center model is expected to decrease, due to a more rapid increase in minimum temperatures, relative to maximum temperatures. This in turn implies the opposite sequence of changes in surface variables to that expected during the summer, and is indicative of the importance of the presence of moisture over southern Africa in the determination of a wide range of climate changes.

MONITORING FOREST COVER AND LAND USE USING SATELLITE IMAGERY

Foster Kwame Mensah

The increasing rate of deforestation in Ghana is significantly affected by agricultural land use change in the forest zone. The driving force behind this has been found to be the pressure exerted on land as a result of the increase in population growth over the years.

The existence of geographically referenced data on the spatial distribution of forested areas as well as associated attributes, such as total acreage of different cover types, and forest inventory data is key to effective monitoring of the forest zone. The use of satellite imagery can provide cost effective means for creating spatial data sets for monitoring and for providing inputs for forest zone decision support systems.

The objective of this project is to produce digital and hard copy maps of the forest cover and of land use in a specified buffer zone for two forest reserves in the eastern part of Ghana, at a scale of 1:30,000. This data set is required for use as part of baseline inventory of forest cover which monitors deforestation areas. The spatial nature of this data set clearly depicts the distribution of land use and of forest cover in the forest ecosystem. By realizing that the spatial fragmentation of forest cover has an effect on ecological processes, it is intended to produce forest cover and land use change for the area of interest and to explore methods for linking the cartographic output to ecological models.

The primary data source for this project was SPOT panchromatic and multi-spectral satellite data.

Appendix 3

African Workshop Group Models

Appendix 3
African Workshop Group Models

Modelling Lake Water Quality In Agro-Eco System

R. Boukchina, S. Jain, W. Goma

A STELLA model was developed to simulate Nitrate concentration in runoff to the natural reservoir (lake) from agriculture watershed. The flow chart of STELLA linked water budget process to nitrogen budget in soil to simulate runoff nitrate exportation to the lake. The hydrological, micro biological, agronomical and hydrolic processes were the basis for the logical and mathematical relationships among the input variables which were rain, evapotranspiration, organic and inorganic fertilizers, field capacity, rate of nitrification and plant uptake. The model was run with two fertilizer scenarios. Results showed that nitrate output can be controlled by the fertilizer application management.

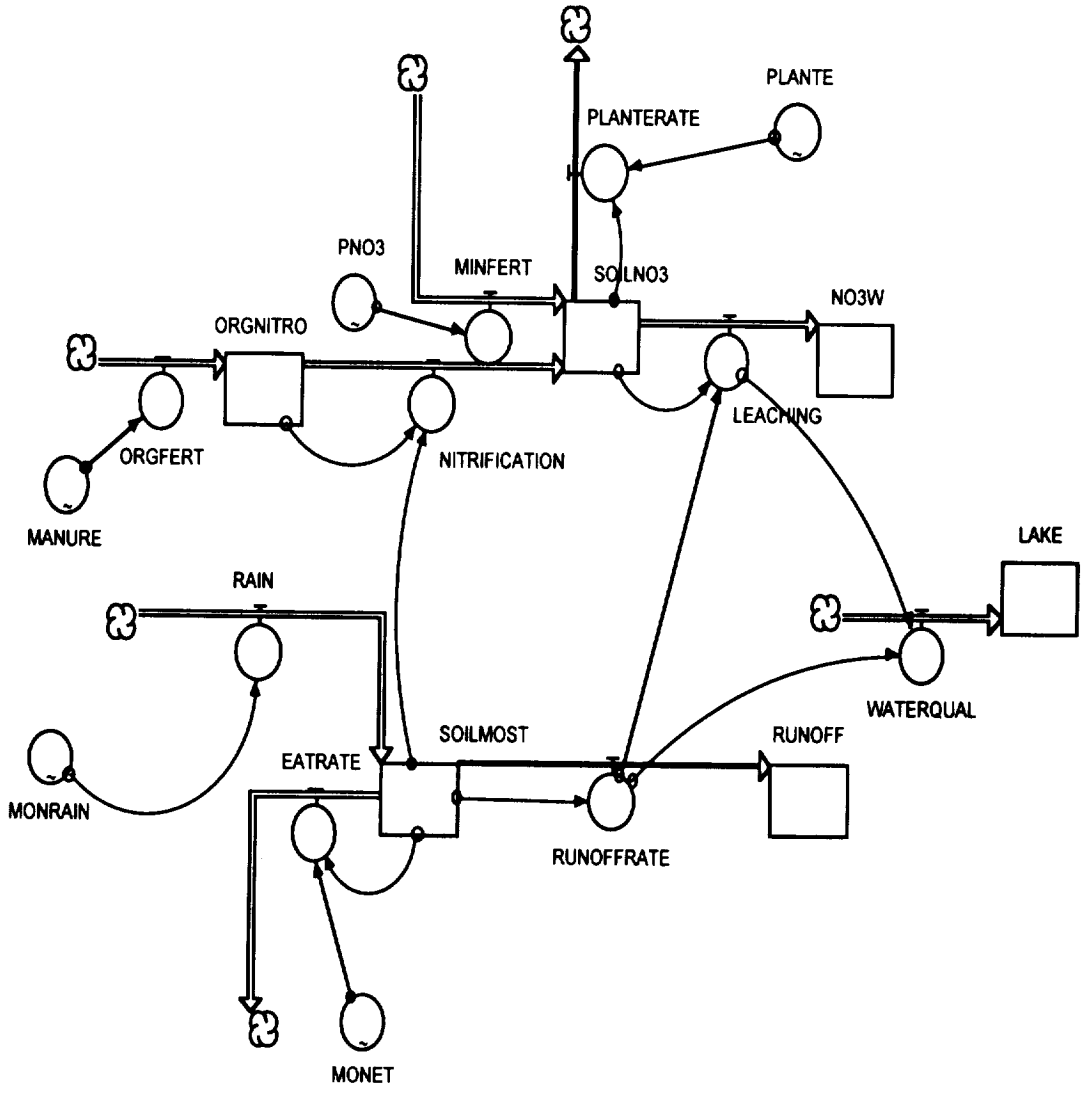

Model For A Community Managed Woodland In Zimbabwe

C. Gumbie, M.B.M. Sekhwela, F.K. Mensah, K.V. Rabah

INTRODUCTION

The development of natural woodlands or forests is influenced by many factors, some of which include fire, drought, harvesting, animal browsing and damage, just to mention a few. The growth of the forest depends on precipitation and natural or artificial regeneration. Human influence can be expressed in terms of the clearing of forest for arable use, cutting for energy, and logging for construction and industrial timber.

Thus interactive relationships can be better depicted or expressed with an ecological model which details inputs to the system, outputs from the system, and flows within the system. Where such relationships can be defined or expressed mathematically, simulation models can be developed to further explore and increase the understanding of such interactive ecosystem processes. This can also help to provide possibilities for predicting the likely outcomes of various management options for sustainable development. An example of this is a simulation model of a community managed natural woodland in a dry Savanna adjacent to a Game Park in Zimbabwe.

Model Conceptualization

The model assumes an existing natural woodland of approximately 5000 hectare, which is exposed to pressure from human-related activities, climatic, and elephant disturbance.

Stage 1: Woodland

An initial stand of 15000 trees is assumed, and managed for a 50 year period. The dynamics of the woodland is dependent on human activities, climatic, regeneration, mortality, and elephant disturbance.

Stage 2: Human Activity

The human component plays a significant role whereby some proportion of the woodland is cleared by the neighboring community for agricultural purpose (15%), harvested for fuel(19%), and for construction and industrial timber(15%). All these activities contribute to tree cutting which lead to tree removal (death).

Stage 3: Tree Mortality

Factors contributing to tree death in this type of woodland are known to be fires and drought. In the model it is assumed that the contribution due to fire is 15% and that to drought is 25%. The contribution of elephant damage also is quite significant, due to the proximity of the woodland to a Game Park.

Stage 4: Elephant Population

The dynamics of elephant population has a direct effect on the woodland system. It is therefore important to control the elephant population through culling, assuming the elephant population grows at a rate of 1% per annum.

Stage 5: Climatic Factor

In the dry Savanna woodland rainfall plays a significant role on vegetation, particularly on seedling development. It is assumed that 25% of the seedlings will survive and be recruited into the woodland system. It is also assumed that some of the trees in the woodland system die through natural thinning.

RESULTS

The seedling and the recruitment levels fluctuated in line with rainfall pattern as expected, as both germination and seedling establishment depend on soil moisture levels. Initially the woodland shows fluctuating disturbances due to elephant damage until the elephant population is reduced by culling to sustainable levels. At this sustainable level both seedling and recruitment are replenishing the woodland stock which appears to stabilize for the next twenty years.

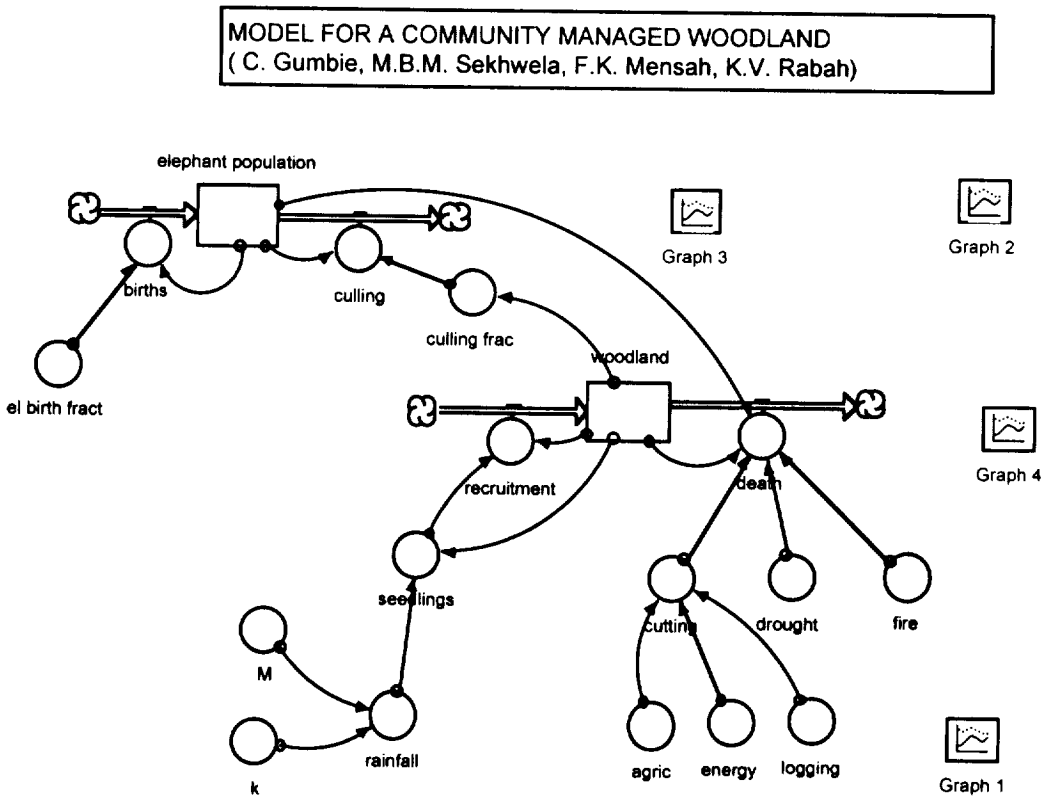

CLIMATE CHANGE AND HUMAN HEALTH WITH STELLA

Presented by P. C. OKE & A. ABDELLAOUI

The objectives of this project are :
- To make an inventory of climate-induced diseases
- To study if conditions of climatic change have modified the disease vectors in terrestrial ecosystems
- To study the interrelation between the prevalence of diseases and climate factors
- To study the impact of climate change/health relation on the socio-economic development
- To build a model for predicting the risk of health decline caused by climate change

The predictive model dealt with one case of disease which correlates with climatic parameters. We have introduced an input Harmattan index, microbe opportunity, immunization condition, nutritional condition, random seed factor. Thus, this rate has permitted us to calculate the population morbidity . In the second trial, we introduced the parameters (discomfort index, treatment, delays, random seed 2) which permitted us to determine the lethality. This model permitted us to simulate the effects of climate parameters on the population submitted to a virulence of microbe.

This model is constituted by three blocks :
- CLIMATIC PARAMETERS
- MORBIDITY MECHANISMS
- MORTALITY MECHANISMS

Each block has several components which are traduced by this diagram.
In this model, there are several sensitivity selectors which permit us to simulate different conditions.
These graphics traduce the results of simulation :
- Graphic 1 : Climate conditions / CSM in state 0.
- Graphic 2 : Climate conditions / CSM in state 1.
- Graphic 3 : Climate conditions / CSM in random state.

This model must be completed by other blocks to integrate other variables. The equations must be corrected to permit the best calibration of the model.

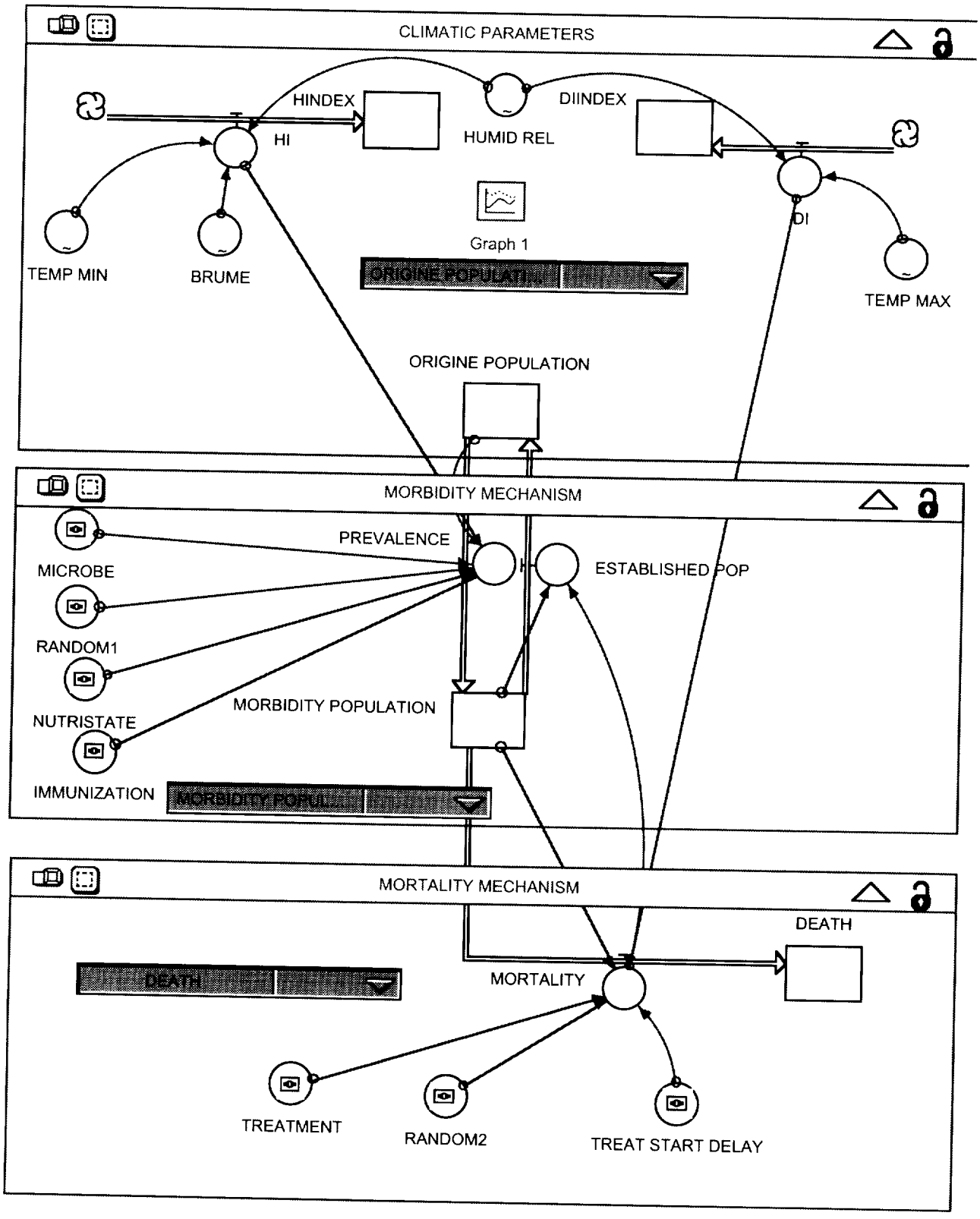
CLIMATIC PARAMETERS
HINDEX
HI
HUMID REL
DIINDEX
DI
Graph 1
TEMP MIN
BRUME
TEMP MAX
ORIGINE POPULATION
ORIGINE POPULATION
MORBIDITY MECHANISM
PREVALENCE
MICROBE
ESTABLISHED POP
RANDOM1
NUTRISTATE
MORBIDITY POPULATION
IMMUNIZATION
MORTALITY MECHANISM
DEATH
DEATH
MORTALITY
TREATMENT
RANDOM2
TREAT START DELAY

MODEL FOR A COMMUNITY MANAGED WOODLAND IN ZIMBABWE

(C. Gumbie, M.B.M. Sekhwela, F.K. Mensah, K.V. Rabah)

Introduction

The development of natural woodlands or forests is influenced by many factors, some of which include fire, drought, harvesting, animal browsing and damage, just to mention a few. The growth of the forest depends on precipitation and natural or artificial regeneration. Human influence can be expressed in terms of the clearing of forest for arable use, cutting for energy, and logging for construction and industrial timber.

Thus interactive relationships can be better depicted or expressed with an ecological model which details inputs to the system, outputs from the system, and flows within the system. Where such relationships can be defined or expressed mathematically, simulation models can be developed to further explore and increase the understanding of such interactive ecosystem processes. This can also help to provide possibilities for predicting the likely outcomes of various management options for sustainable development. An example of this is a simulation model of a community managed natural woodland in a dry Savanna adjacent to a Game Park in Zimbabwe.

Model Conceptualization

The model assumes an existing natural woodland of approximately 5000 hectare, which is exposed to pressure from human-related activities, climatic, and elephant disturbance.

Stage 1: Woodland

An initial stand of 15000 trees is assumed, and managed for a 50 year period. The dynamics of the woodland is dependent on human activities, climatic, regeneration, mortality, and elephant disturbance.

Stage 2: Human Activity

The human component plays a significant role whereby some proportion of the woodland is cleared by the neighboring community for agricultural purpose (15%), harvested for fuel(19%), and for construction and industrial timber(15%). All these activities contribute to tree cutting which lead to tree removal (death).

Stage 3: Tree Mortality

Factors contributing to tree death in this type of woodland are known to be fires and drought. In the model it is assumed that the contribution due to fire is 15% and that to drought is 25%. The contribution of elephant damage also is quite significant, due to the proximity of the woodland to a Game Park.

Stage 4: Elephant Population

The dynamics of elephant population has a direct effect on the woodland system. It is therefore important to control the elephant population through culling, assuming the elephant population grows at a rate of 1% per annum.

Stage 5: Climatic Factor

In the dry Savanna woodland rainfall plays a significant role on vegetation, particularly on seedling development. It is assumed that 25% of the seedlings will survive and be recruited into the woodland system. It is also assumed that some of the trees in the woodland system die through natural thinning.

Results

The seedling and the recruitment levels fluctuated in line with rainfall pattern as expected, as both germination and seedling establishment depend on soil moisture levels. Initially the woodland shows fluctuating disturbances due to elephant damage until the elephant population is reduced by culling to sustainable levels. At this sustainable level both seedling and recruitment are replenishing the woodland stock which appears to stabilize for the next twenty years.

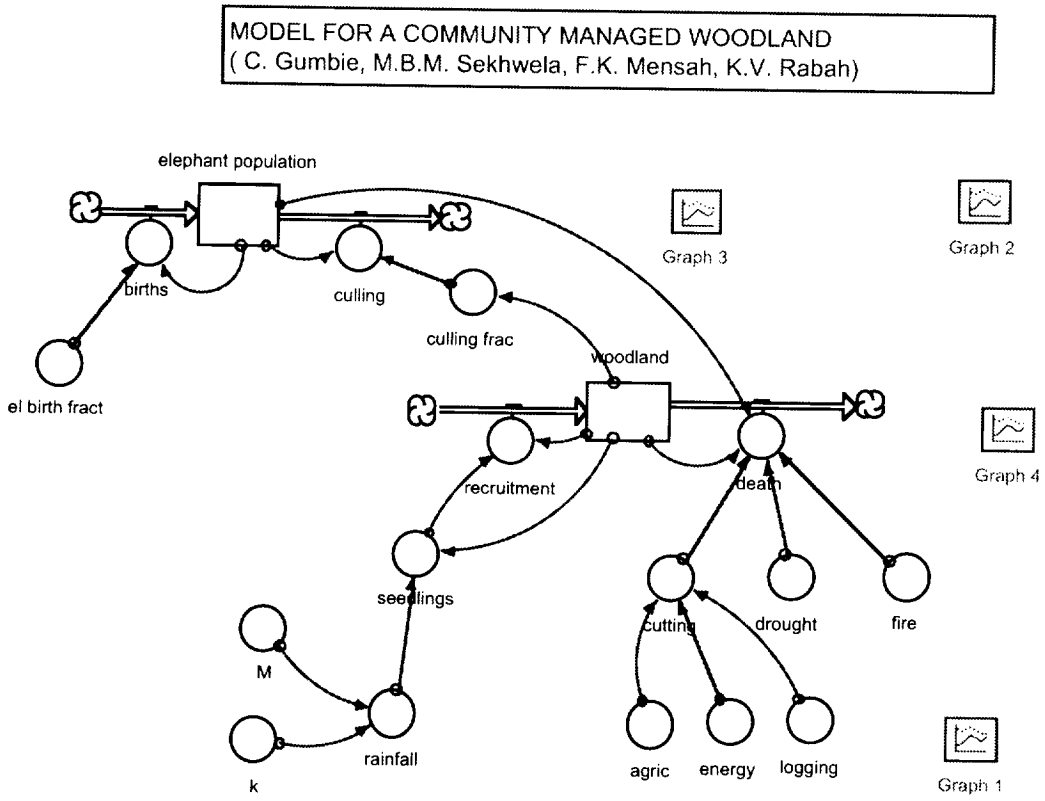

MODELLING THE POTENTIAL HYDROLOGICAL IMPACTS OF CLIMATE CHANGE OVER TWO SITES IN SOUTH AFRICA

Alec Joubert
Climatology Research Group, University of the Witwatersrand

Introduction

Estimates of climate change based on general circulation models (GCMs) are available for Africa south of the equator (defined below as southern Africa). Point estimates for two climatically-distinct sites in South Africa have been used as inputs to the ACRU model in order to investigate the potential hydrological impacts of regional climate change. The two sites selected are near Cape Town (a winter rainfall region) and north of Pretoria (a summer rainfall region).

The aims of the project are to model the potential hydrological impacts of expected climate changes on two climatically-distinct sites in South Africa. In particular, the objective of the study is to identify the relative sensitivities of simulated total stream flow (runoff) and soil moisture in the first soil layer (A-horizon) to imposed climate change. In addition, we aim to develop familiarity with the ACRU modeling system, and particularly to improve the understanding of the sensitivity of the hydrological cycle to exceed on ACRU by means of adjustments to mean monthly maximum and minimum temperatures. Regardless of the sign of change in DTR, the magnitude of the change was limited to 1°C (in keeping with GCM estimates).

For the summer rainfall site, summer and autumn DTRs (September-May) were increased by 1°C by imposing a 2°C increase in maximum temperature and a 1°C increase in minimum temperature. During winter (June-August), the DTR was decreased by 1°C by imposing a 2°C increase in minimum temperature and a 1°C increase in maximum temperature. For the winter rainfall site, the DTR was decreased by 1°C throughout the year (as described for winter above).

Sites

Two climatically-distinct sites have been selected: Elsenburg, situated in a winter rainfall region near Cape Town; and Roodeplaat, situated in a summer rainfall region north of Pretoria. Daily rainfall series for both sites were estimated using the stochastic rainfall generator within the ACRU model. The use of stochastic rainfall series implies that inter-annual and intra-annual variability of rainfall at the actual sites is slightly under-estimated. A correction was applied to these data using the PPTCOR multiplication factor within ACRU to adjust the median monthly rainfall of the stochastic rainfall series to that of the actual station.

Mean monthly maximum and minimum temperatures were estimated by the author to represent the actual observed time series. No actual data were available at the workshop.

Imposed Climate Changes

The GCM-derived changes in regional climate are based on those models which provide the most reliable estimates of regional climate change. In all cases, the imposed changes probably represent a conservative estimate of the changes which are most likely to occur regionally. For each site, two simulations were run. The first represents a control simulation, in which no climate changes were imposed. Climate changes as described below were imposed for a second simulation at each site. The imposed changes include:

Rainfall:
Austral (Southern Hemisphere) seasons are used below. Mean monthly rainfall for the both the early and late summer seasons (September-February) as well as the late summer and autumn (March-May) were decreased by 10 percent. During the winter months (June-August), mean monthly rainfall was increased by 10 percent. These changes represent the consensus of a wide range of GCM projections and were applied at both stations. The ACRU model provides a decomposition of mean monthly rainfall to daily time series internally, by means of Fourier analysis.

Diurnal Temperature Ranges:
Changes in diurnal temperature range (DTR) were imposinear response of the hydrological system to relatively small changes in mean monthly rainfall. The changes in total stream flow at the winter rainfall site are smaller (on a percentage basis) than those at the summer rainfall site possibly indicating a different hydrological

response on the basis of rainfall intensity. Rainfall resulting from convective thunderstorms may be expected to be more intense, than rainfall resulting from frontal systems, and this may be expected to cause the difference in runoff response at the two sites. Soil moisture changes in the A-soil horizon are less than 1 mm/month throughout the year, suggesting again that changes in soil moisture are more conservative than changes in runoff.

Preliminary Results

Winter Rainfall Region:
The annual rainfall cycle at Elsenburg exhibits are marked winter-season peak . The perturbed rainfall used to simulated anthropogenically-induced climate change does not alter the shape of the annual cycle, although its amplitude is affected. The primary mode of rainfall production at this site is frontal. The 10% decrease in winter rainfall results in a reduction of approximately 10 mm/month . During summer, the 10% increase in rainfall results in an increase of approximately 2 mm/month.
Percentage changes in total stream flow (runoff) are similar to those for rainfall (approximately 10% in winter). However, these changes represent only a 3-5 mm/month change in the magnitude of runoff . Runoff changes in during summer are much smaller than during winter, given the generally lower rainfall. Changes in soil moisture in the A-soil horizon are very small (less than 1 mm/month) throughout the year, representing a change of less than 5% in all months . Therefore in all cases the changes in soil moisture are smaller than the changes in rainfall imposed in the perturbed simulation.

Summer Rainfall Region:
The summer rainfall site (Roodeplaat) also exhibits a strong annual rainfall cycle, with a pronounced summer rainfall maximum. Mean monthly rainfall throughout the winter months is less than 10 mm/month. The primary mode of rainfall production over this region is convective.
The change in mean monthly rainfall induced in the perturbed simulation resulted in a decrease of summer rainfall by approximately 10 mm/month, but negligible changes in mean rainfall during winter. The annual cycle in total stream flow (runoff) also reflects a strong annual cycle, with very little runoff during the winter months.

The changes in total stream flow simulated in the perturbed experiment result in a 2-3 mm/month decrease in runoff during the summer months, and a change of less than 1 mm/month during winter. The changes in total stream flow during summer represent a decrease of approximately 30% over the control simulation, and are indicative of the highly non-expected climate change.

Summary and Conclusions

This study has indicated the sensitivity of hydrological systems to relatively conservative (small) changes in mean climate. At both the summer and winter rainfall sites used in the present study, the changes in mean rainfall are unlikely to have important climatological implications. However, the highly non-linear response of total stream flow at Roodeplaat during summer is indicative of the potential for considerable hydrological implications resulting from those small changes in rainfall. Importantly, the hydrological response of a system is (among others) a function of soil type, mode of rainfall production (as a control on rainfall intensity), and antecedent conditions (what is the existing soil moisture content?). The potential exists in future to extend this preliminary study to other regions of South and southern Africa, and to examine the potent hydrological implications of other climate changes, for example those related to expected changes in the frequency and magnitude of extreme rainfall events.

Prediction of Soil Loss in the Sub-humid Tropics Using the STELLA Model

O. Totolo, P. Yanda, D. Olago and E. Sambo

Introduction

Soil erosion is a problem in most countries of the world. The process seriously impacts on the productivity and usefulness of the land. The aerial coverage of the land is seriously reduced by gullies and other erosion features. Soil erosion also impacts negatively on the aesthetic beauty of the land. It is therefore of paramount importance to try to understand this insidious process.

One way to understand the process of soil erosion is to try to understand the interactions and interrelationships of the input parameters and their ultimate influence on the output parameters. However, input parameters (data) are limited in most of African countries. Such relationships between variables can therefore be achieved through extrapolation and interpolation of limited data. This is made possible by creating models or using the available models. In this exercise, STELLA was used to create a model to explain the interactions and interrelationships of the input parameters and to also predict the output parameters affected by one or more parameters. This is very useful because given a set of parameters, the model enables you to forecast a number of scenarios which could be helpful in land management and policy decisions. Modeling enables scientists to experiment with different situations and in this way, policy makers and land managers can make well informed decisions on the basis of modeling results.

Objectives

1. estimate soil loss in the sub-humid area in the tropics
2. establish levels of influence on soil loss for each of the variables
3 develop different scenarios on measures to mitigate soil loss

Figure 1: Conceptual Framework for Soil Erosion Model

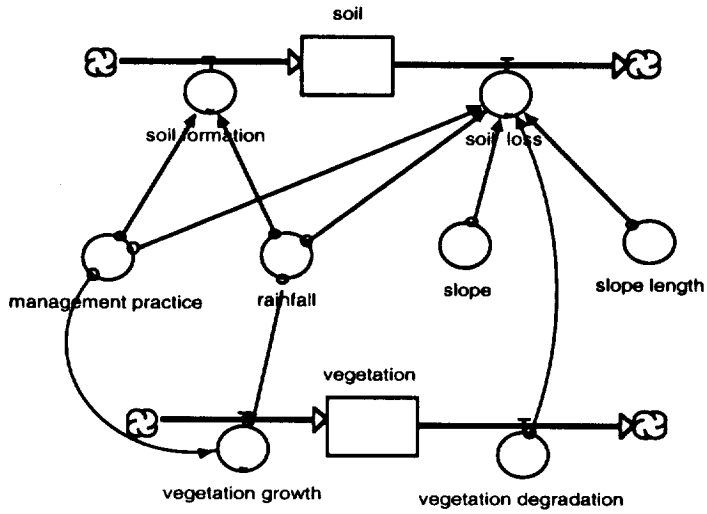

Figure 2: Relationship between soil loss, vegetation degradation, vegetation growth and rainfall

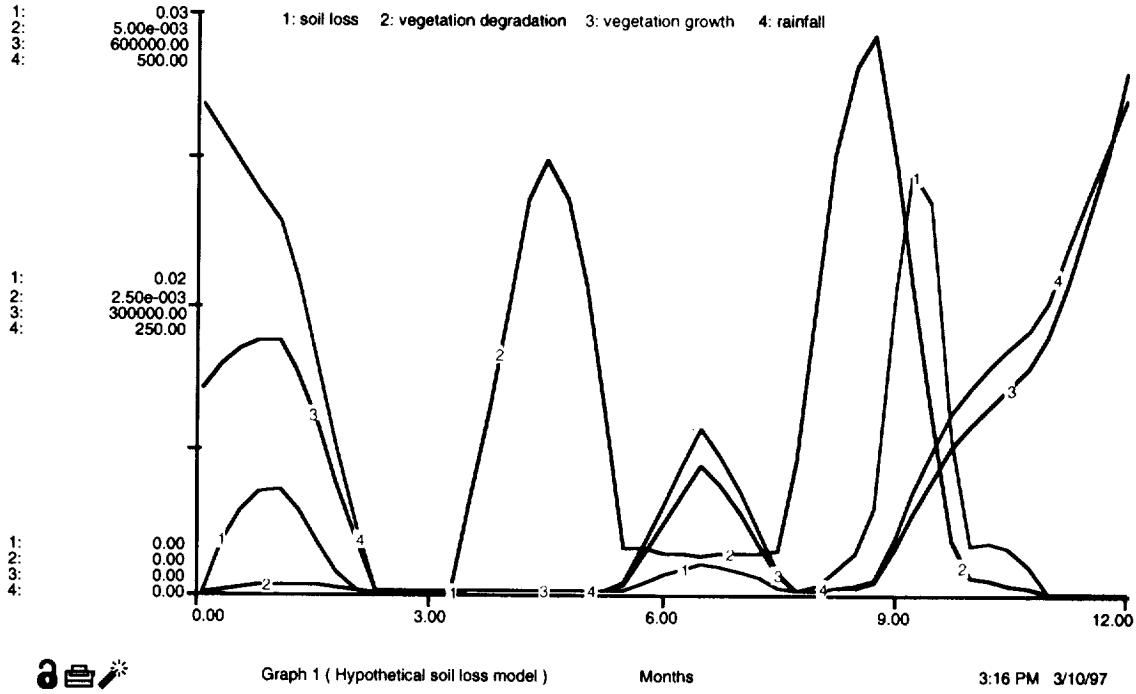

Description of relationships between variables used in the model

soil(t) = soil(t - dt) + (soil_formation - soil__loss) * dt
INIT soil = 500
soil_formation = soil_management*rainfall
soil__loss = vegetation_degradation*slope*slope_length*rainfall*soil_management
vegetation(t) = vegetation(t - dt) + (vegetation_growth - vegetation_degradation) * dt
INIT vegetation = 500
vegetation_growth = rainfall*soil
vegetation_degradation = harvesting*fire*grazing
harvesting = if(vegetation>500)then(.000000000001*vegetation)else(0)
slope = 1/500
slope_length = 200
fire = GRAPH(time)
(0.00, 0.05), (1.09, 0.05), (2.18, 0.00), (3.27, 0.00), (4.36, 2.80), (5.45, 0.15), (6.55, 0.1), (7.64, 0.1), (8.73, 2.45), (9.82, 0.05), (10.9, 0.00), (12.0, 0.00)
grazing = GRAPH(time)
(0.00, 7350), (1.09, 6100), (2.18, 5450), (3.27, 2900), (4.36, 3000), (5.45, 5900), (6.55, 6050), (7.64, 5800), (8.73, 3300), (9.82, 3350), (10.9, 5950), (12.0, 6950)
rainfall = GRAPH(time)
(0.00, 420), (1.09, 313), (2.18, 2.50), (3.27, 2.50), (4.36, 0.00), (5.45, 2.50), (6.55, 148), (7.64, 0.00), (8.73, 7.50), (9.82, 165), (10.9, 238), (12.0, 428)
soil_management = GRAPH(time)
(0.00, 0.935), (1.09, 0.525), (2.18, 0.4), (3.27, 0.14), (4.36, 0.095), (5.45, 0.09), (6.55, 0.085), (7.64, 0.1), (8.73, 0.205), (9.82, 0.29), (10.9, 0.43), (12.0, 0.95)

Future Plans

It is envisaged that this project will be extended to other parts of Africa to cover as many climatic zones as possible. Initially the project will select sites in Kenya, Tanzania, Malawi and Botswana. A comparative study will be made to determine the parameters that should be incorporated within the STELLA model. Cross-model comparisons will be made with, for example, ACRU, HYDRO and CENTURY. Apart from the vegetation modeling that has been initiated at the workshop, there is also interest in erosion aspects.

Land Cover Changes on Zomba Mountain and Impacts on Water Yields in the Mulunguzi Catchment

Paul V. Desanker, Eston Y. Sambo, Geoffrey Chavula

Background

The Zomba Mountain Catchment area of the Mulunguzi River and Dam has provided drinking water to the town of Zomba for many years. Good data, covering a period of 40 years or more, for runoff exists from a gauging station just before the Mulunguzi River flows into the Mulunguzi Dam at the edge of the Zomba Mountain. From around 1908-1920, the Department of Forestry has converted indigenous vegetation over most of the mountain to highly productive pine, cypress and Mulanje cedar plantations (*Pinus patula, Cupressus lustanica, Widringtonia nodiflora).* The forests are managed on a clear-cutting cycle regardless of slope. Fires and wind have also taken their toll recently in creating drastic cover changes. Siltation is also a major problem and the dam had to be dredged in the late 1980's when it almost dried out. Water yields from the mountain have diminished to crisis levels (University of Malawi and schools have changed schedules, water is rationed as a matter of routine, etc.). Other possible reasons advanced for water shortages in the Zomba Municipality have included the presence of a crack in the base of the dam, leading to loss of reservoir water, or changes in climatic patterns that have resulted in increased drought incidences. In this study, we hypothesize that the aforestation program has modified the water balance to a point that water yields have been adversely affected, compounded by poor land management leading to siltation problems.

Mulunguzi dam lies in a catchment of around 18 km2 on Zomba plateau (one of four main catchments for Lake Chilwa, an inland drainage lake). The dam was originally constructed for electricity generation for Zomba town in the 1940's when the population was less than 10,000 but it has now grown to over 50,000. There are plans to start construction of a new dam upstream beginning 1997/98. This is expected to further change the hydrological characteristics.

Overall Goal

Quantify water balance components in relation to land cover types over the Mulunguzi River catchment and apply results to forest scheduling and collection dam dynamics.

Specific Objectives

1. Calculate water balance of the Mulunguzi basin and compare with gauge data
2. Reconstruct a hypothetical time series of forest cover (forest cover types, etc.) for the Zomba Mountain Forest Reserve to provide inputs of the vegetation component in the hydrological model.
3. Relate forest cutting patterns to water yields and attempt to optimize spatial patterns to maximum water yields.

Related Studies

- IGBP/LUCC Miombo Network.
- Study on the management of the Lake Chilwa Basin by the Biology Department, University of Malawi (possibly to be funded by DANIDA).
- GAIM Working Group on Sedimentation - Effectiveness of the different cover types in trapping sedimentation

Design of the study

The catchment will be divided into land cover types or compartments which will form units of 5-10 hectare in size:

- Forest plantation (conifer) - various age/size classes
- Grassland
- Woodland (indigenous) - *miombo*, etc
- Bare ground after clear felling

The historical data will characterize land cover changes in the periods:

- Prior to 1900 : grassland and *miombo*
- 1900 ~ 1920 : small areas planted with conifers
- 1920 ~ 1950 : about half of the plateau planted to conifers
- 1950 - present: whole mountain covered in forest on a 15-25 year rotation. The management is on a clear-cut regime including the slopes.

Modelling

- The ACRU model will be run for cover types as sub-catchments and runoff accumulated in the dam.
- A time series will be constructed for land cover type distributions for the whole area from 1900 - now at 20 year intervals.
- A sedimentation model will be run to cover the history of the dam.

Expected Results

The models are expected to provide information to answer questions on how the hydrological cycle has been impacted by the aforestation program. An important outcome will be to see how the present forest cutting patterns relate to water yields compared with other management regimes. This may provide ideas on how to optimize spatial patterns to maximize water yields.

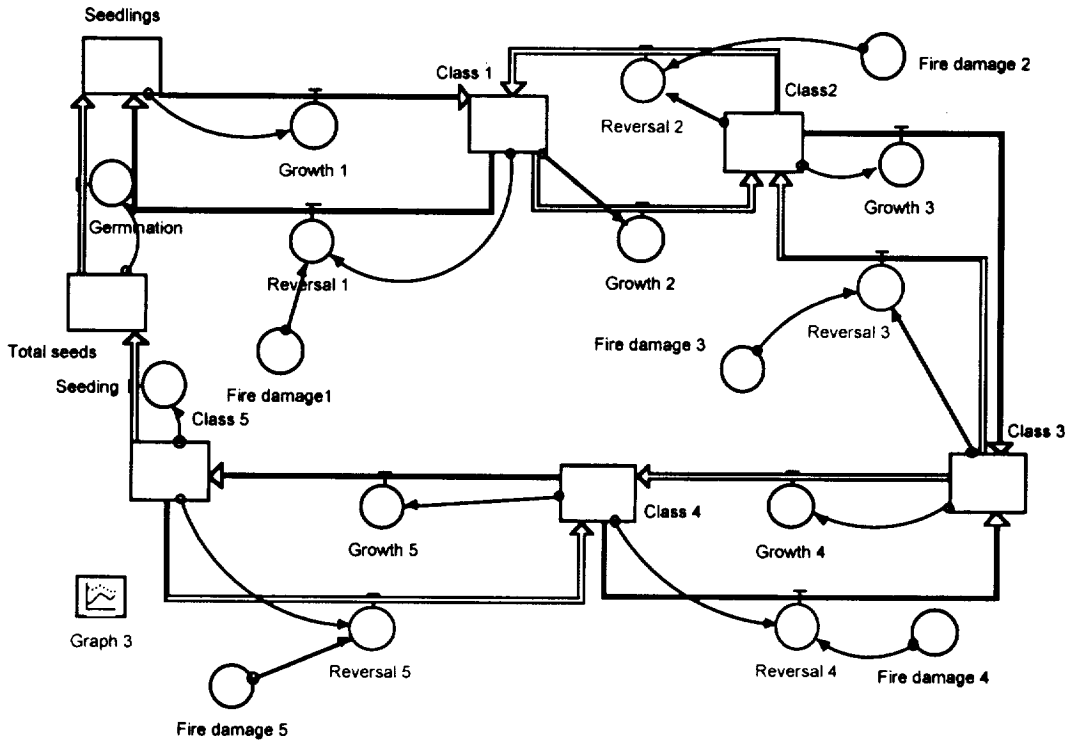

Effects of fire on population dynamics of Teak woodlands

STELLA model of atmospheric emissions in Togo
A. Ajavon

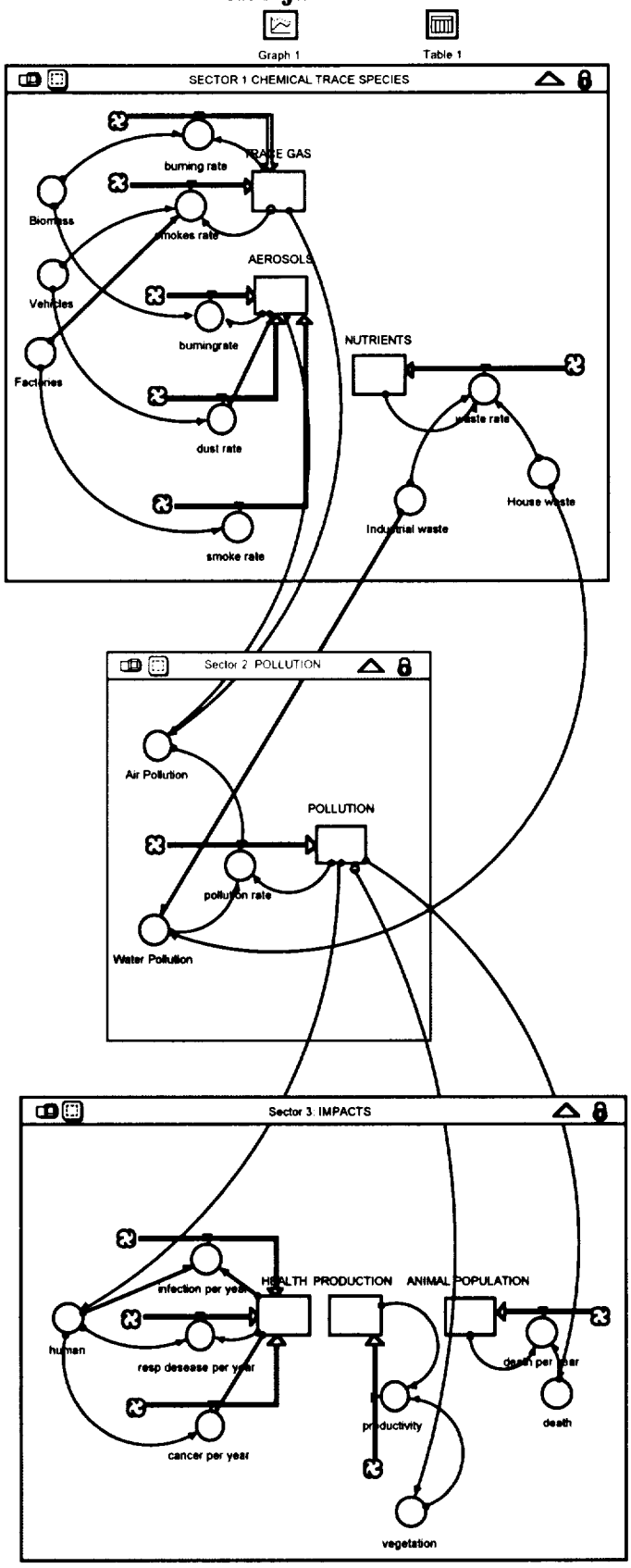

REFERENCES

Bacastow, R., and G.R. Stegen, Estimating the Potential for CO2 sequestrian in the ocean using a carbon cycle model, *presented adn 91i in Honolulu*, 1991.

Banse, K., and D.C. English, Seasonality of Coastal Zone Color Scanner Phytoplankton Pigment in the Offshore Oceans, *J. of Geophysical Research--Oceans*, *99*, 7323-7345, 1994.

Bolin, B.B., E.T. Deegens, S. Kempe, and P. Ketner, The global carbon cycle, New York, 1979.

Bolin, B.B., B.R. Doos, J. Jager, and R. Warrick, *The Greenhouse Effect, Climate Change, and Ecosystems*, 541 pp., John Wiley & Sons, Chichester, 1986.

Broecker, W., T. Peng, G. Ostlund, and M. Stuiver, The distribution of bomb radiocarbon in the ocean, *J. Geophys. Res.*, *90*, 6953-6970, 1985.

Ciais, P., P. Tans, J. White, M. Trolier, D. Schimel, and others, Partitioning of Ocean and Land Uptake of CO2 as Inferred by Delta-C-13 Measurements from the NOAA Climate Monitoring and Diagnostics Laboratory Global Air Sampling Network, *J. Geophys. Res.*, *100*, 5051-5070, 1995.

Conkright, M.D., and E.K. Asem, Global Ionosperic Effects of the October 1989 Geomagnetic Storm, *Journal of Geophysical research-Space Physics*, *99*, 6201-6218, 1995.

Cramer, W., IGBP Newsletter, Workshop on globally gridded historical climate data sets for biosphere models., 1996.

Cramer, W., M. Hutchinson, R. Leemans, and B. Huntley, A new climate data base for terrestrial ecosystem modelling with variable spatial resolution, in prep.

Cramer, W., B. Moore, and D. Sahagian, Data needs for modelling global biospheric carbon fluxes - lessons from a comparison of models. IGBP Newsletter, 1996.

Friend, A., Parameterisation of a global daily weather generator for terrestrial ecosystem and biogeochemical modelling, *Ecological Modelling*, in press.

Fung, I., C. Tucker, and K. Prentice, Application of advanced very high resolution radiometer vegetation index to study atmosphere biosphere exchange of CO2., *Journal of Geophysical Research*, *92*, 2999-3015, 1987.

Hubert, B., L. Francois, P. Warnant, and D. Strivay, Stochastic generation of meteorological variables and effects on global models of water and carbon cycles in vegetationand soils, *Journal of Hydrology*, in press.

Hulme, M., Rainfall changes in Africa: 1931-1960 1961-1990, *International Journal of Climatology*, *12*, 685-699, 1992.

Keeling, C., J. Chin, and T. Whorf, Increased activity of northern vegetaion inferred from atmospheric CO2 measurements, *Nature*, *382*, 146-148, 1996.

Keeling, C., T. Whorf, M. Wahlen, and J.v.d. Plicht, Interannual extremes in the rate of rise of atmospheric carbon dioxide since 1980, *Nature*, *375*, 666-670, 1995.

Kurz, K.D., and E. Maier-Reimer, Iron Fertilizaton of the austral ocean-- The Hamburg Model Assessment, *Global Biogeochem. Cycles*, *7*, 229-244, 1993.

Leemans, R., and W. Cramer, The IIASA database for mean monthly values of temperature, precipitation, and cloudiness on a global terrestrial grid, IIASA, 1991.

Levin, I., and V. Hesshaimer, Refining of Atmospheric Transport Model Entries by the Globally Observed Passive Tracer Disbributions of (85)Krypton and Sulfur Hexafluoride (SF6), *J. of Geophysical Research--Atmospheres*, *101*, 16745-16755, 1996.

Levitus, S., and T.P. Boyer, *World Ocean Atlas 1994*, , NOAA Atlas NESDID 4, NODC, , Washington, D.C., 1994.

Maier-Reimer, E., U. Mikolajewicz, and A. Winguth, Future Ocean Uptake of CO2--Interaction Between Ocean Circulation and Biology, *Climate Dynamics*, *12*, 711-721, 1996.

Maiss, M., and I. Levin, Global Increase of SF6 Observed in the Atmosphere, *Geophysical Research Letters*, *21*, 569-572, 1994.

Maiss, M., L.P. Steele, R.J. Francey, P.J. Fraser, and e. al, Sulfur Hexafluoride--A Powerful New Atmospheric Tracer, *Atmospheric Environment*, *30*, 1621-1629, 1996.

Manabe, S., and R.J. Stouffer, Multiple-Century Response of a Coupled Ocean-Atmosphere Model to an Increase of Atmospheric Carbon Dioxide, *Journal of Climate*, *7*, 5-23, 1994.

Meeson, B., F. Corpew, and J. McManus, Initiative I-global Data Sets for Land-atmosphere Models, NASA, 1995.

Melillo, J., I. Prentice, G. Farquhar, E. Schulze, and O. Sala, Terrestrial Biotic Responses to Environmental Change and Feedbacks to Climate, in *Climate Change 1995- The Science of Climate Change*, edited by J. Houghton, L.M. Filho, B. Callander, N. Harris, A. Kattenberg, and K. Maskell, pp. 445-481, Cambridge University Press, Cambridge, 1996.

Moore III, B., R. Boone, J. Hobbie, R. Houghton, J. Melillo, B. Peterson, G. Shaver, C. Vorosmarty, and G. Woodwell, A simple model for analysis of the role of terrestrial ecosystmes in the global carbon budget, in *Modelling the global carbon cycle*, edited by B. Boiln, pp. 365-385, Wiley, N.Y., 1981.

Moore III, B., and B. Braswell, The Lifetime of Excess Atmospheric Carbon Dioxide, *Global Biogeochemical Cycles*, *8*, 23-38, 1994.

Najjar, R.G., and R.F. Keeling, Analysis of the mean annual cycle of the dissolved oxygen anomaly in the World Ocean, *Journal of Marine Research*, *55*, 117-151, 1997.

Najjar, R.G., J.L. Sarmiento, and J.R. Toggweiler, Downward transport and fate of organic matter in the ocean: simulations with a general ocean circulation model, *Global Biogeochemical Cycles*, *6*, 45-76, 1992.

Olson, D., and S. Prince, Global primary production data initiative update, *IGBP Newsletter*, *27*, 13, 1996.

Orr, J., and J. Sarmiento, Potential of Marine Macroalgae as a Sink for CO2 - Constraints from a 3-D General Circulation Model of the Global Ocean, *Water, Air, Soil Pol.*, *64*, 405-421, 1992.

Otto, R., E. Hunt, and G. Kohlmaier, Static and dynamic input data of Terrestrial Biogeochemical Models, *GLobal Biogeochemical Cycles*, manuscript.

Prince, S., R. Olson, G. Dedieu, G. Esser, and W. Cramer, Global Primary Production Data Initiative Project Description, IGBP DIS, 1995.

Rayner, P., and R. Law, A comparison of modelled responses to prescribed CO2 sources, CSIRO Division of Atmospheric Research, 1995.

Ruimy, A., G. Dedieu, and B. Saugier, TURC: a diagnostic model of continental gross primary productivity and net primary productivity., *Global Biogeochemical Cycles*, *10*, 269-286, 1996.

Sarmiento, J., and J. Orr, 3-D Simulations of the Impact of Southern Ocean Nutrient Depletion on Atmospheric CO2 and Ocean Chemistry, *Limn. and Ocean.*, *36*, 1928-1950, 1991.

Sarmiento, J., J. Orr, and U. Siegenthaler, A Perturbation Simulation of CO2 Uptake in an Ocean General Circulation Model, *J. Geophys. Res.*, *97*, 3621-3645, 1992.

Sarmiento, J.L., and C. LeQuere, Oceanic Carbon Dioxide Uptake in a Model of Centruy-Scale Global Warming, *Science*, *274*, 1346-1350, 1996.

Schimel, D., Terrestrial Ecosystems and the Carbon Cycle, *Glob. Change Bio.*, *1*, 77-91, 1995a.

Schimel, D.S., Terrestrial Biogeochemical Cycles: Global Estimates with Remote Sensing, *Remote Sens. Environ.*, *51*, 49-56, 1995b.

Scholes, B., The global soil task, *IGBP Newsletter*, *27*, 10, 1996.

Sellers, P.J., C.J. Tucker, G.J. Collatz, S.O. Los, C.O. Justice, D.A. Dazlich, and D.A. Randall, A global 1 degree by 1 degree NDVI data set for climate studies. Part 2: The generation of global fields of terrestrial biophysical parameters from the NDVI, *Int.J. Remote Sensing*, *15*, 3519-3545, 1994.

Siegenthaler, U., and J. Sarmiento, Atmospheric Carbon Dioxide and the Ocean, *Nature*, *365*, 119-125, 1993.

Takahashi, T., R.A. Feely, R.F. Weiss, R.H. Wanninkhof, and e. al, Global air-sea flux of CO2: An estimate based on measurements of sea-air pCO(2) difference, *Proceedings of the National Academy of Sciences of the United States of America*, *94*, 8292-8299, 1997.

Takahashi, T., and S. Sutherland, An assessment of the role of the North Atlantic as a CO2 sink, *Phil. Trans. R. Soc. Lond.*, *B348*, 143-152, 1995.

Tans, P., I. Fung, and T. Takahashi, Observational constraints on the global atmospheric CO2 budget, *Science*, *247*, 1431-1438, 1990.

Turner, B.L., D.L. Skole, S. Anderson, G. Fischer, L. Fresco, and R. Leemans, Land Use and Land-Cover Change: Science/Research Plan, *IGBP*, *35*, 1995.

Volk, T., Multi-property modeling of ocean basin carbon fluxes, *nasa contractor report*, 1988.

Watson, A.J., Volcanic iron, CO2, ocean productivity and climate, *Nature*, *385*, 587-588, 1997.

Yoder, J.A., C.R. McClain, G.C. Feldman, and W.E. Esaias, Annual Cycles of Phytoplankton Chlorophyll Concentrations in the Global Ocean--A Satellite View, *Global Biogeochemical Cycles*, *7*, 181-193, 1993.